



**HAL**  
open science

## A concise guide to modelling the physics of embodied intelligence in soft robotics

Gianmarco Mengaldo, Federico Renda, Steven L Brunton, Moritz Bächer, Marcello Calisti, Christian Duriez, Gregory S Chirikjian, Cecilia Laschi

### ► To cite this version:

Gianmarco Mengaldo, Federico Renda, Steven L Brunton, Moritz Bächer, Marcello Calisti, et al.. A concise guide to modelling the physics of embodied intelligence in soft robotics. *Nature Reviews Physics*, 2022, 4 (9), pp.595-610. 10.1038/s42254-022-00481-z . hal-03921606

**HAL Id: hal-03921606**

**<https://inria.hal.science/hal-03921606>**

Submitted on 3 Jan 2023

**HAL** is a multi-disciplinary open access archive for the deposit and dissemination of scientific research documents, whether they are published or not. The documents may come from teaching and research institutions in France or abroad, or from public or private research centers.

L'archive ouverte pluridisciplinaire **HAL**, est destinée au dépôt et à la diffusion de documents scientifiques de niveau recherche, publiés ou non, émanant des établissements d'enseignement et de recherche français ou étrangers, des laboratoires publics ou privés.

# A concise guide to modeling the physics of embodied intelligence in soft robotics

Gianmarco Mengaldo<sup>1\*</sup>, Federico Renda<sup>2</sup>, Steven L. Brunton<sup>3</sup>, Moritz Bächer<sup>4</sup>, Marcello Calisti<sup>5</sup>, Christian Duriez<sup>6</sup>, Gregory S. Chirikjian<sup>1</sup> and Cecilia Laschi<sup>1\*</sup>

<sup>1</sup>National University of Singapore, Singapore, SG.

<sup>2</sup>Khalifa University, Abu Dhabi, UAE.

<sup>3</sup>University of Washington, Seattle, USA.

<sup>4</sup>Disney Research, Zurich, Switzerland.

<sup>5</sup>University of Lincoln, Lincoln, UK.

<sup>6</sup>INRIA, Lille, France.

\*Corresponding author(s): [mpegim@nus.edu.sg](mailto:mpegim@nus.edu.sg); [mpeclc@nus.edu.sg](mailto:mpeclc@nus.edu.sg);

Contributing authors: [federico.renda@ku.ac.ae](mailto:federico.renda@ku.ac.ae); [sbrunton@uw.edu](mailto:sbrunton@uw.edu);

[moritz.baecher@disneyresearch.com](mailto:moritz.baecher@disneyresearch.com); [mcalisti@lincoln.ac.uk](mailto:mcalisti@lincoln.ac.uk);

[christian.duriez@inria.fr](mailto:christian.duriez@inria.fr); [mpegre@nus.edu.sg](mailto:mpegre@nus.edu.sg);

## Abstract

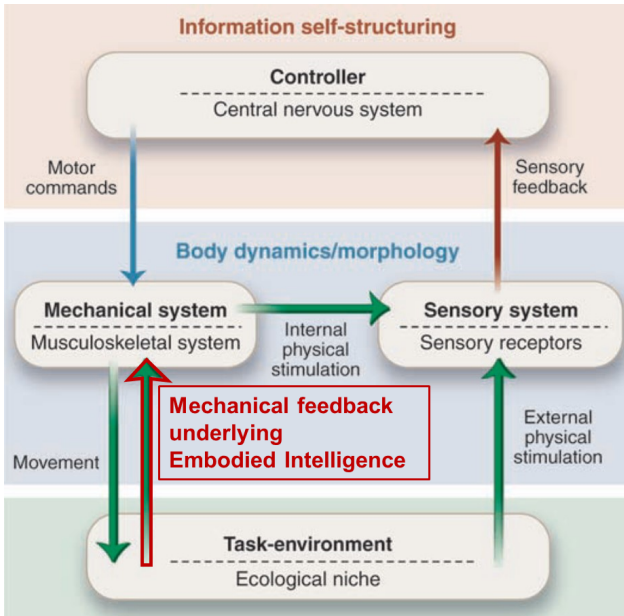
Embodied intelligence, or intelligence that requires and leverages a physical body, is ubiquitous in biological systems, both in animals and plants. Through embodied intelligence, biological systems efficiently interact with and use their surrounding environment to let adaptive behaviour emerge. In soft robotics, this is a well-known paradigm, whose mathematical description and consequent computational modelling remain elusive. We argue that filling this gap will enable full uptake of embodied intelligence in soft robots. The resulting models can be used for design and control purposes. In this [paper](#), we provide a concise guide to the main mathematical modelling approaches, and consequent computational modeling strategies, that can be used to describe soft robots and their physical interactions with the surrounding environment, including fluid and solid media. The goal of this perspective is to convey the challenges and opportunities within the context of modeling the physical interactions underpinning embodied intelligence. We emphasize that interdisciplinary work is required, especially in the context of fully coupled robot-environment interaction modeling. Promoting this dialogue across disciplines is a necessary step to further advance the field of soft robotics.

36 **Keywords:** Soft robotics, Embodied intelligence, Mathematical modeling,  
37 Computational modeling, Computational physics

## 38 1 Introduction

39 Soft robotics is largely motivated by the functional role of soft tissues in liv-  
40 ing organisms [1]. Life has had millions of years to adapt to its surrounding  
41 environment and co-evolve nervous and muscle-skeletal systems to achieve  
42 task-efficient performance, synergistically. We observe that living beings are  
43 soft and compliant, and we argue that this is instrumental to their embodied  
44 intelligence [2]. According to this modern view of intelligence, the phys-  
45 ical body play a much larger role in shaping intelligence, since a part of  
46 sensory–motor behaviour emerges from its interaction with the surrounding  
47 environment, with minimal or no involvement of the nervous system. Soft bio-  
48 logical systems use their complex internal body structure to efficiently leverage  
49 physical interactions with the external environment and achieve the desired  
50 actions. Indeed, external interaction forces, instead of being treated as distur-  
51 bances needing compensation, are used for the intended movements [3]. As an  
52 example, in locomotion, gravity is exploited for stepping forward, and adapta-  
53 tion to uneven terrains is provided by compliant elements within the leg joints,  
54 with limited need for active inputs from the central nervous system. Similarly,  
55 octopuses, an iconic model for soft robotics, adopt highly effective unfolding  
56 arm reaching movements by leveraging the buoyancy and interaction forces  
57 from the water surrounding them.

58 Embodied intelligence is a well-known paradigm in robotics and in soft  
59 robotics. In a typical robot sensory–motor behaviour scheme, we can consider  
60 a sensory system perceiving the environment, controllers processing the incom-  
61 ing information and planning a motor action, and then a mechanical system  
62 that executes motor actions in the physical environment. Embodied intelli-  
63 gence can be seen as the mechanical feedback from the environment, directly  
64 onto the mechanical system of the robot physical body, with no involvement  
65 of controllers or processing (see Fig. 1, from [2]). This view gives a clear per-  
66 ception of how powerful embodied intelligence can be in simplifying robot  
67 sensory–motor behaviour and increasing overall robot efficiency and effective-  
68 ness. All this works if we assume that a soft, compliant body receives, and  
69 does not reject, the mechanical feedback from the environment.



**Fig. 1:** In a typical sensory–motor scheme, either for a robot or a biological system, three main components are usually considered: a sensory system (receptors in biology) receiving inputs from the external environment, some form of controller (nervous system in animals), and a mechanical system (musculoskeletal system in biology) acting on the environment for accomplishing a task. Embodied intelligence can be seen as the mechanical feedback received by the physical body from the environment. It involves the body dynamics and morphology with no involvement of the controller. It allows closing a very short control loop, by-passing most of the computational processes. (Reprinted with permission from [2] and adapted).

70 How to systematically design embodied intelligence into soft robots is one of  
 71 the current challenges in the field of soft robotics. We argue that this goal can  
 72 be achieved by means of a mathematical description of the physical interactions  
 73 characterizing embodied intelligence. Related computational modeling would  
 74 enable simulations to be used for both design and control purposes.

75 The task of constructing this modeling framework is not an easy one. We  
 76 focus on the soft parts that are necessary to implement embodied intelligence  
 77 and that go beyond the rigid-body modeling techniques used in robotics. Take  
 78 as an example a soft arm immersed in a fluid and interacting with solids (see,  
 79 e.g., the octopus in Fig. 2). To describe and model the physics underlying  
 80 embodied intelligence, it is necessary to consider:

- 81 • the continuous deformations of the arm deriving from muscle activations,

- the coupled interaction of the arm with the fluid, when e.g., the arm reaches out for target objects and moves the fluid, and the fluid contributes to its deformation,
- the interactions of the soft arm with solids (rigid or deformable), like the seafloor when walking, or external objects when grasping.

The description of these three points present a number of significant challenges.

First, the problem is inherently multiphysics, due to the physically heterogeneous nature of interactions underlying embodied intelligence. In fact, one needs to take into account the physics of the soft body and the dynamics of muscle activation, the flow physics and its coupling with the soft body, and the physics describing contact and adhesion between two solids. This poses the critical challenge (and opportunity) of interdisciplinary work across multiple communities, ranging from robotics, fluid dynamics, structural mechanics, tribology, and contact mechanics. These fields typically have their own customs and terminology, and cross-fertilization can prove difficult, yet will be beneficial to bring advances in modeling embodied intelligence.

Second, the problem is multiscale, as the number of scales one needs to describe may range from millimeters to meters. For instance, in our example the arm reaching movement may undergo an overall displacement of several centimeters. Yet, the description of the deformation of the soft body, and its interaction with the flow and solid, may require a much finer description to accurately capture its behaviour. To this end, fast computational methods to solve multiscale problems are required. Integration with the scientific computing and applied mathematics communities may therefore prove important.

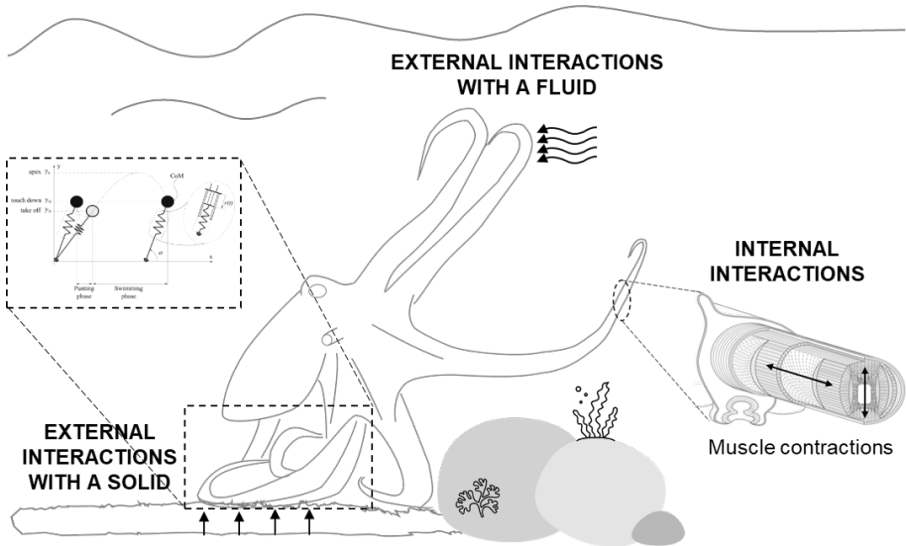
Multiphysics and multiscale problems are notoriously challenging but have successfully been conquered in some fields, including the aerospace industry, biomedical engineering, and material science, to cite a few. In these fields, it may be possible to develop a *digital twin*, which is a virtual representation of the system comprised of a hierarchy of models for different components and levels of fidelity, ultimately pinned to data [4, 5]. In the context of soft robotics, these problems have yet to be addressed, although promising advances have been made. Some of the factors that make modelling particularly difficult here are: i) how the actuation forces are designed and mathematically modelled to achieve a desired action, and how the surrounding environment influences them; ii) large deformations of nonlinear materials and their coupled interactions with the surrounding medium, which lead to high-dimensional models that are often prohibitively expensive to simulate and use inside control loops; and iii) partially known interfacial physics and unmodeled dynamics – e.g., nonlinear friction mechanisms for solid–solid interaction, and turbulent drag for fluid–structure interaction. In addition, the range of morphologies (e.g., arms, fingers, legs, fins), materials (e.g., hyperelastic, heterogeneous, functional), abilities (e.g., reaching, grasping, walking, morphing, growing, swimming, jumping, crawling, digging) and

127 intended applications (e.g., healthcare, manufacturing, underwater sensing and  
128 manipulation, scientific exploration, entertainment) is extremely diverse, exac-  
129 erbating the complexity of the modelling task. The latter aspect may lead  
130 to staggered and application-specific modelling strategies, that may not be  
131 beneficial to the soft robotics field.

132 In this paper, to support our argument of distilling embodied intelligence  
133 into physical interactions, we provide a concise guide to the latter and to their  
134 underlying mathematical models. In particular, we present and discuss the  
135 most prominent models that describe 1) the interactions of soft robot compo-  
136 nents (including actuators) that lead to efficient movements and deformation,  
137 and 2) the robot interactions with the surrounding environment. We refer to  
138 the former as *internal interactions*, and the latter as *external interactions*,  
139 where the environment can be constituted by a fluid or a solid.<sup>1</sup> To introduce  
140 the models underlying the physical interactions found in embodied intelligence,  
141 we use the octopus depicted in Fig. 2 as a proxy for a general biological or  
142 soft robotics system. The octopus represents an excellent model for soft-body  
143 parts, while not excluding rigid components in the overall treatment of the  
144 problem. Analogously, we consider interaction with a general fluid, which holds  
145 for liquids as well as gases. The description of the modeling techniques has  
146 the aim of providing the basic tools for their uptake. To this end, we give a  
147 comprehensive picture, including both internal and external interactions, both  
148 with solids and fluids. We also showcase their use and discuss the challenges  
149 that can promote beneficial interdisciplinary interactions.

---

<sup>1</sup>We note that the surrounding environment may be constituted of heterogeneous granular material. In this case, one may need to rely on different methods than the ones presented in this paper. Yet, the case of solid or fluid media is sufficiently general to provide an effective guide on modeling interactions between soft bodies and the environment.



**Fig. 2:** An illustration of our scope in modeling the physics of embodied intelligence. We use an octopus as a proxy for a general soft body, in its environment, where we highlight the three key modeling areas that contribute to a substantial insight of embodied intelligence: *internal interactions*, and *external interactions* models, either with a fluid medium or a solid support. Internal interactions refer to the deformations of the soft body induced by actuators, or muscles. External interactions refer to the action of the external environment (fluid or solid) on the soft body. We also highlight how the accurate description of internal and external interactions can lead to low-dimensional models that capture the soft body behaviour with a reduced number of state variables.

## 150 1.1 A Mathematical Framework for Modeling of Soft Robots

The mathematical framework adopted belongs to the realm of mechanics that is at the foundations of physical interactions in both solids and fluids. To describe the mechanics of physical systems there are two views, Lagrangian and Eulerian. In the former, one tracks the trajectories of particles, while in the latter one observes the particle velocities at a fixed point in space. The Lagrangian setting is commonly used in classical solid mechanics, while the Eulerian setting is commonly used in fluid mechanics. These two views allow us to introduce an abstract mathematical formalism for the soft body subject to

*internal* and *external* interactions that consists of a set of differential equations:

$$\mathcal{D}\mathbf{q}_{\text{sb}} = \mathcal{N}_{\text{sb}} + \mathcal{C}_{\text{int}} + \mathcal{C}_{\text{ext}}, \quad \text{in } \Omega_{\text{sb}}. \quad (1)$$

Equation (1), along with suitable initial and boundary conditions, can describe both models arising in continuum mechanics and multibody dynamics in the soft body domain  $\Omega_{\text{sb}}$ . The former typically yields a set of partial differential equations, while the latter a set of ordinary differential equations. Depending on the approach used, the variables  $\mathbf{q}_{\text{sb}}$ , that describe the soft body (sb), can have a different meaning. For instance, in a Lagrangian view,  $\mathbf{q}_{\text{sb}}$  represents the position and momentum of material particles, while in an Eulerian view,  $\mathbf{q}_{\text{sb}}$  is the observed velocity at each given point.  $\mathcal{D}$  is a differential operator that may be a partial ( $\partial$ ) or a total (d) derivative (including a material derivative D), of first or second order.

$\mathcal{N}_{\text{sb}}$  is a nonlinear term that describes the soft body (sb) mechanics, which may depend on  $\mathbf{q}_{\text{sb}}$ , its partial derivatives with respect to spatial coordinates  $\mathbf{x}$ , time  $t$ , and by a set of tunable constants such as viscosity, stiffness, and other actuation and material parameters.

$\mathcal{C}_{\text{int}}$  is a coupling term that accounts for internal (int) interactions (e.g., actuation forces for tendons or pressure of pneumatic chambers).  $\mathcal{C}_{\text{ext}}$  is a coupling term that accounts for external (ext) interactions (e.g., contact with external solids or interactions with the surrounding medium).

While equation (1) may not be the standard way of introducing models in the realm of soft robotics, it allows a sufficiently general mathematical framework that can be used as a basis to construct a unified formalism for the multiphysics of internal and external interactions. We divided the right-hand side into a nonlinear term  $\mathcal{N}_{\text{sb}}$ , and two coupling terms  $\mathcal{C}_{\text{int}}$  and  $\mathcal{C}_{\text{ext}}$ , to emphasize the mechanics of the soft body (through  $\mathcal{N}_{\text{sb}}$ ) and its coupling not only with internal (through  $\mathcal{C}_{\text{int}}$ ) but also with external systems (through  $\mathcal{C}_{\text{ext}}$ ). In particular,  $\mathcal{C}_{\text{int}}$ , and  $\mathcal{C}_{\text{ext}}$  can constitute forcing terms, that results from lumping the interactions into simplified terms, or can be terms coupling the equation describing the soft body (1) to additional equations describing the physics of internal and/or external interactions (e.g., actuators, and the surrounding environment). These interactions could be for instance described by equality and inequality constraints, especially when the soft body is in contact with a medium. In this case, the constraints can be embedded into the equations by means of, e.g., Lagrange multipliers, and encapsulate the physics of interactions. For example, frictional contact between two surfaces is best modeled with inequality constraints which become active as soon as a soft body is in contact with either itself or the environment.

Starting from equation (1), in the following we introduce the models and solution methods adopted for *internal* and *external* interactions. More specifically, the outline of this paper is as follows. In section 2, we detail the models for internal interactions, describing both the models for soft-body mechanics (i.e.,  $\mathcal{N}_{\text{sb}}$ ), and the internal interactions with actuators (i.e.,  $\mathcal{C}_{\text{int}}$ ). In section 3, we



192 describe the models for external interactions (i.e.,  $\mathcal{C}_{\text{ext}}$ ). In section 4, we outline  
193 how these models can be used in practice for soft robotics, such as by lever-  
194 aging reduced order models. In section 5, we review the modeling challenges  
195 and opportunities described, and draw some conclusions and perspectives.

## 196 2 Internal interactions

### 197 2.1 Challenges

198 A soft-bodied system, such as the arm of the octopus depicted in Fig. 2, is  
199 composed of a set of sensors and actuators, distributed inside a soft tissue,  
200 that work together to achieve a given task. The various sensing and actuation  
201 mechanisms interact internally with one another, and they typically oper-  
202 ate within a nonlinear and possibly heterogeneous material constituting the  
203 soft tissue. We focus here on the fundamental robotics task of modeling the  
204 relations between the actuator space and the soft-body deformations. A math-  
205 ematical model describing internal interactions should therefore capture the  
206 robot deformation (i.e.,  $\mathcal{N}_{\text{sb}}$ ) produced by the internal actuation forces, where  
207 the latter also needs to be accurately represented (i.e.,  $\mathcal{C}_{\text{int}}$ ).

208 The physics of actuation corresponds to a subset of the total degrees of  
209 freedom of the system, associated to the physics of deformation of the struc-  
210 ture. Once the subspace of actuation is defined, the key challenges specific to  
211 modeling internal interactions are:

- 212 1. to model the physics of the actuation in such a way that it can be identified  
213 on the real system, and
- 214 2. to couple the two physics: the one of the deformation of the structure, and  
215 the one of the actuation.

216 In terms of actuation, we take into account the following three main  
217 strategies

218 **Tendons (1D).** We consider a punctual action of a cable or similar tendon-  
219 like actuator, that can be considered as one-dimensional (1D). If the tension  
220 is exerted by a tendon which pulls, it is relatively easy to describe the force  
221 field created on a soft robot structure, based on the geometrical path. When  
222 a series of tendons are placed on a robot and their input lengths need to be  
223 integrated, the problem becomes more complex: since the tendons are coupled,  
224 it is necessary to verify that they are tense to exert a force. The tension of  
225 one tendon on a structure could slack on other ones. Also the tension inside  
226 the tendon is a signed force: we can pull with a tendon, but not push. The  
227 algebraic equations, translating the motion of the tendon, lead to constraints  
228 of inequality and complementarity. Finally, more advanced models that could  
229 be used to replicate the mechanics of the tendons (extension, bending, internal  
230 friction, etc.) are neglected to focus on this tensile force.

231 **Flexible fluidic actuators (2D).** We consider chambers that deform when  
232 pressurized with a fluid, so that pressure acts on a surface, and is assumed

233 to be constrained to two-dimensional (2D) deformations. In the same way, for  
 234 these fluidic actuators, it is possible to directly take into account the pressure  
 235 exerted in cavities. This pressure is then integrated on the surface of the cavity  
 236 to calculate a force field applied to the soft robot structure. This approach  
 237 is often used for pneumatic actuation, based on pressure regulators. On the  
 238 other hand, in the case of liquid injection, it is often the variation of the cavity  
 239 volume to constitute the input of the model. As with the tendon case, it is then  
 240 necessary to add an algebraic equation in the model translating the volume  
 241 variation. Moreover, the weight exerted by the liquid on the structure can  
 242 create additional deformations. Finally, one can imagine, in the longer term,  
 243 coupling the deformation models with dynamic models of the fluid.

244 **Smart materials** (3D). We consider a large class of materials responding  
 245 to external stimuli that can be regarded as three-dimensional (3D) actu-  
 246 ators. Some smart materials, such as electro-active or electro-ionic polymers,  
 247 have their internal stress field dependent on an electric field. Other materi-  
 248 als, such as shape memory materials, have their constitutive law dependent  
 249 on temperature. Materials can also be integrated into soft robots that react  
 250 to a magnetic field. In all these cases (and possibly in many others, the field  
 251 of smart material being vast), the problem is the coupling of the deformation  
 252 equations with other equations of physics, like electric or magnetic fields or  
 253 temperature diffusion, often at scales that are much smaller than the scale of  
 254 the robot.

255 The modeling of these actuators constitutes a challenge *per se*, and their inte-  
 256 gration with different soft-body models can be non-trivial. In particular, soft  
 257 robots are highly under-actuated (the degrees of freedom associated with actu-  
 258 ation are significantly fewer than the degrees of freedom of the soft body).  
 259 Therefore, it is frequently required to add algebraic constraints, often associ-  
 260 ated with Lagrange multipliers  $\mathbf{\Lambda}$  and  $\mathbf{\Theta}$ , to drive the motion of the soft body  
 261 within the actuator space. In this case, the coupling term with the actuators  
 262 becomes  $\mathcal{C}_{\text{int}} = \mathbf{\Lambda}^T \mathcal{I}_e + \mathbf{\Theta}^T \mathcal{I}_i$ , where  $\mathcal{I}_e$  and  $\mathcal{I}_i$  are equality and inequality  
 263 constraints, respectively. The method of the Lagrange multipliers is a strategy  
 264 to enforce equality constraints to a functional, in this case equation (1).

## 265 2.2 Models

266 Two modeling approaches of internal interactions exist in robotics. The first,  
 267 called direct modeling approach, starts from the knowledge of the motion  
 268 and/or forces in the actuator space and from other unactuated degrees of  
 269 freedom to compute the robot shape. The second, known as inverse modeling  
 270 approach, starts from a desired shape or position of the robot and calculates  
 271 the actuator space in order to reach the desired shape/position.

272 In this section we will focus on the direct modeling approach. The actuator  
 273 forces will modify the static equilibrium or the dynamics of the robot.

274 In the following, we introduce the main models that can be used for  
 275 describing the soft body mechanics  $\mathcal{N}_{\text{sb}}$  and how they can be integrated with

276 the actuation strategies reported above, through  $\mathcal{C}_{\text{int}}$ . We introduce contin-  
 277 uum solid mechanics models (fully 3D or rod/shells) and finite-dimensional  
 278 parametrization models and we keep their description at a level general enough  
 279 to provide the reader with tools adaptable to most cases. We also introduce  
 280 the possible use of data-driven methods for the same modelling problems.

### 281 *2.2.1 Continuum three-dimensional solid mechanics models*

282 The most general model that captures the full complexity of the soft body is  
 283 given by three-dimensional continuum solid mechanics (see Fig. 3(a)). If we  
 284 consider equation (1), taking an Eulerian view:

285  $\mathcal{D}$  becomes  $\partial/\partial t$ , the partial derivative with respect to time  $t$ ,  
 286  $\mathbf{q}_{\text{sb}}$  becomes  $\mathbf{v}_{\text{sb}}$ , representing the velocity field of the soft body,  
 287  $\mathcal{N}_{\text{sb}}$  becomes  $\nabla \cdot \boldsymbol{\sigma}_{\text{sb}}$ , the divergence of the soft body stress tensor  $\boldsymbol{\sigma}_{\text{sb}}$ .

288 This equation describes the balance of linear momentum, that is usually com-  
 289 plemented by the balance of angular momentum, through  $\boldsymbol{\sigma} = \boldsymbol{\sigma}^T$ , and  
 290 balance of mass, through  $\partial\rho/\partial t + \rho(\nabla \cdot \mathbf{v}_{\text{sb}}) = 0$ . One can also consider adding  
 291 the balance of energy. The constitutive relations for describing the soft-body  
 292 material usually rely on both elastic and hyperelastic models, or ad-hoc con-  
 293 stitutive models. These ad-hoc constitutive relations can originate from e.g.,  
 294 phenomenological experiments of a specimen and provide an accurate simula-  
 295 tion of the soft body deformation [6]. Note that hyperelastic models sometimes  
 296 have many parameters that are difficult to identify in practice. Moreover, other  
 297 phenomena such as viscosity, plasticity or anisotropy need also to be consid-  
 298 ered into the constitutive equations. Anisotropy has, for example, a direct  
 299 influence on the kinematics of the soft robot [7]. Finally, these deformation  
 300 models are very sensitive to the boundary conditions, thus to the modeling of  
 301 the actuators but also to external interactions.

302 All the three actuation strategies, tendons, fluidic actuators, and smart  
 303 materials, can be adopted in conjunction with continuum solid mechanics.  
 304 Their coupling with the soft body is obtained through the term  $\mathcal{C}_{\text{int}}$ . This can  
 305 be constituted by Lagrange multipliers  $\mathcal{C}_{\text{int}} = \mathbf{\Lambda}^T \mathcal{I}_e + \mathbf{\Theta}^T \mathcal{I}_i$  arising from a set  
 306 of constraints imposed by the actuators on the soft body. They can also be  
 307 imposed as a set of boundary conditions for equation (1).

308 Solution strategies rely on numerical methods, e.g., finite and spectral ele-  
 309 ment methods, whereby the partial differential equations are solved at a set  
 310 of prescribed nodes (or mesh). This is typically extremely expensive compu-  
 311 tationally with a corresponding number of degrees of freedom in the order of  
 312  $\mathcal{O}(N^3)$ , where  $N$  is the number of nodes of the underlying mesh. Indeed, a con-  
 313 vergent solution (i.e., a solution that provides the correct results) depends on  
 314 the number and type of elements chosen as well as on their geometric quality,  
 315 where complex geometrical features and nonlinearities might further influence  
 316 the solution convergence. The requirements in terms of solution convergence  
 317 might also differ depending on the way boundary conditions are applied – i.e.,  
 318 the convergence of one or another variable might be required. For instance, if

319 we consider a fluid (liquid or gas) which inflates a cavity, and we load the cavity  
320 in volume (thanks to a constraint), then the convergence of the motion vari-  
321 ables (position and velocity) is sufficient. However, if the structure is loaded  
322 in pressure, it must be in equilibrium with the stress variables of the material,  
323 hence, the convergence of stresses is needed. In addition, for the management  
324 of contacts with e.g., internal actuation systems, it is sometimes necessary  
325 to use a finer mesh on the surface of the objects in order not to alter their  
326 geometric definitions, thus undermining the accuracy of the simulation.

327 Successful implementations in the realm of soft robotics applications exist.  
328 The software *SOFA* implements the finite element method to simulate con-  
329 tinuum solid mechanics [8], and offers solutions, such as model reduction [9],  
330 to find a compromise between accuracy and computation time. Fig. 4-(a)  
331 shows an example of its use for modeling a soft pneumatic finger. *ChainQueen*  
332 implements a differentiable Lagrangian-Eulerian physical simulator based on  
333 the moving least square material point method for solid mechanics, along  
334 with actuation and contact with external objects [10]. *Evosoro* uses a solid  
335 mechanics engine, *Voxelyze* [11], that allows the simulation of soft multi-  
336 material robots [12]. These three options are open-source and currently under  
337 active development. Some additional commercial software to tackle the internal  
338 interaction modeling challenge exist, including *ABAQUS* [13], *ANSYS* [14],  
339 *COMSOL* [15], and *Altair* [16], among others. These provide platforms for  
340 solving full complexity solid mechanics problems, but they are not tailored to  
341 soft robotics.

342 This modeling approach, along with the computational strategies for solv-  
343 ing it, allows the description of all topologies commonly required in soft  
344 robotics, e.g., rods, lattice of beams, shells, volumes. These topologies can be  
345 generated by means of Computer-Aided Design (CAD), and standard meshing  
346 practices. This however, may lead to an inexact geometrical representation of  
347 the soft body, that in turn can yield an inaccurate solution for the soft-body  
348 motion. This drawback could be addressed by using accurate mesh genera-  
349 tion practices (e.g., high-order mesh generation [17, 18]) and by increasing the  
350 number of mesh nodes, or with isogeometric analysis [19].

351 We finally note that the framework of 3D continuum mechanics allows  
352 for the description of robots with both soft and rigid components. To couple  
353 soft and rigid body components, soft-body degrees of freedom at the interface  
354 between the soft and rigid part can be expressed as rigid body position and  
355 orientation, or coupling constraints may be introduced [20, 21].

### 356 **2.2.2 Shell and rod models**

357 A significant number of soft robots are characterized by an elongated structure  
358 with two dimensions much smaller compared to the third one. In this case,  
359 it is possible to greatly reduce the number of degrees of freedom required to  
360 describe the robot by adopting 1D rod models. Sometimes, only one dimension  
361 is negligible, and 2D shell models may be adopted. These fall under the realm  
362 of continuum mechanics although not in 3D.

363 A particularly useful continuum modeling approach to describe rods and  
 364 shells in soft robotics is the Cosserat model. In this model, the 3D Boltzmann  
 365 continuum with pointwise three (translational) degrees of freedom is replaced  
 366 by a set of infinitesimal 6D micro-solids stacked along the dominant dimen-  
 367 sions [22]. This intrinsic theory allows simulating the nonlinear finite rotation  
 368 of rods and shells with better accuracy and efficiency compared to approaches  
 369 deduced from a 1D or 2D reduction of the traditional 3D theory [23]. For  
 370 instance, 3D FEM corotational methods leads to a linearization of the kine-  
 371 matic equations that is found unsuitable for the analysis of arbitrarily large  
 372 rigid-body displacements [24].

373 The mathematical formalism underlying a Cosserat model relies on the Lie  
 374 group of rigid body transformation  $SE(3)$ , due to the assumptions made on the  
 375 material microstructures. Following [25], if we consider rods, a Cosserat rod is  
 376 modeled by a continuous set of rigid cross sections stacked along a material  
 377 line parameterized by a curvilinear coordinate  $\mathbf{x} = X \in [0, 1]$  to which a cross-  
 378 sectional frame  $\mathcal{F}(X) = (O, t_1, t_2, t_3)(X)$  is attached, where  $O(X)$  is on the  
 379 midline,  $t_1(X)$  is a unit normal vector perpendicular to the cross-section, and  
 380  $t_2(X)$  and  $t_3(X)$  are the unit vectors spanning the cross-sectional plane (see  
 381 Fig. 3(b)).

382 The balance of momentum underlying this model can be recast within  
 383 equation (1), where:

384  $\mathcal{D}$  becomes  $\partial/\partial t$ , the partial derivative with respect to time  $t$ ,  
 385  $\mathbf{q}_{sb}$  becomes  $[v, \omega]^T$ , the velocity twist field of the soft-body composed of  
 386 the linear and angular velocity, respectively,  
 387  $\mathcal{N}$  becomes  $[\mathcal{N}_{sb,v}, \mathcal{N}_{sb,\omega}]$ , with  
 388  $\mathcal{N}_{sb,v} = 1/(\rho A)(\partial n/\partial x + \bar{n})$ , and  
 389  $\mathcal{N}_{sb,\omega} = (I^{-1}/\rho)(-\omega \times (\rho I \omega) + \partial c/\partial X + \partial r/\partial X \times n + \bar{c})$ .

390 In the above equations,  $\rho$  is the density of the medium,  $I$  is the moment of  
 391 inertia,  $A$  is the area of the cross section,  $r$  is the position vector of  $O(X)$ ,  
 392 while  $n$  and  $c$  are the linear and angular cross-sectional stresses along the  
 393 beam. Fig. 4-(b) shows the application of the method in a soft robot with soft  
 394 appendices for propulsion in water.

395 Tendon and thin fluidic actuators can be easily modeled in this framework  
 396 as active internal wrenches  $\mathcal{C}_{int}$  that act directly on the cross-sectional stress.  
 397 Similar equations can be derived for Cosserat shells [26]. This modeling frame-  
 398 work is not suitable for inflated chambers and some kind of smart material  
 399 actuations, that inherently require a 3D description of the soft body.

400 Solution strategies for Cosserat-like models require the use of numerical  
 401 methods, as they belong to the realm of continuum mechanics. To this end,  
 402 methods introduced in the previous section are all suitable, i.e., finite and  
 403 spectral element methods, and they are usually formulated in generalized coordi-  
 404 nates. It is worth noticing that Cosserat models, regardless of the resolution  
 405 strategy, are well suited to hybrid soft-rigid systems since the kinematics of

both, rigid bodies and Cosserat material points, take values in  $SE(3)$ . Furthermore, more recently a serial, strain-based parametrization of the Cosserat rod has been proposed that seamlessly extend the traditional modeling approach of tree-like rigid robots to hybrid soft-rigid system [27].

In addition to the many research papers based on the Cosserat approach, a few software and toolboxes have been proposed recently to solve the related equations. *Elastica* [28] is a free and open-source software, which provides a discrete differential geometry approximation of the Cosserat rod model. *SoRoSim* [29] is a MATLAB toolbox that implements a strain-parametrization of soft robotic arms. A piecewise-constant strain approximation has also been included as a plug-in in *SOFA* [21].

Although Cosserat-like rod and shell models guarantee a good accuracy for soft robots with one or two main dimensions (e.g., slender bodies) undergoing finite deformation, they are not suitable for full 3D soft robot body deformations.

### 2.2.3 Finite-dimensional parametrization models

The previous models derive from continuum solid mechanics, therefore they lead to sets of partial differential equations, as described in sections 2.2.1 and 2.2.2, that are computationally expensive to solve. It is also possible to describe the behaviour of the soft body via finite dimensional models. These rely on a description of the soft body that leverages a suitably parametrized central axis or “backbone curve”, that assumes a prescribed expression. This description leads to sets of ordinary differential equations in contrast to partial differential equations produced by the previous two modeling strategies.

The parametrization of the backbone curve can be defined as follows. Each frame  $\mathcal{F}(X)$  described in the previous section can be viewed as an element of the group of special Euclidean transformations (i.e., rigid-body displacements). The origin of this frame traces out the backbone curve as the curvilinear coordinate  $X$  varies. The tangent to this curve is the normal to the cross-sectional plane,  $t_1(X)$  (see Fig. 3(c)). For each fixed value of time, the combined rigid-body instantaneous translational and rotational rate of change with respect to arclength is defined by matrix  $\Theta(X) = [\mathcal{F}(X)]^{-1}(\partial\mathcal{F}(X)/\partial X)$  where  $\mathcal{F}(X)$  is the roto-translational matrix describing the orientation and translation of the frame (relative to the world frame at the base of the robot), with components  $\mathbf{R}(X)$  and  $\mathbf{p}(X)$ , respectively [30–32]. In the case when the backbone curve is inextensible (not stretchable), then there is coupling between the rotation matrix and the position vector. For instance, if the tangent to the soft robot arm at its base is  $\mathbf{e}_1 = [1, 0, 0]^T$ , then the tangent at  $X$  will be  $\mathbf{R}(X)\mathbf{e}_1$  and integrating the tangent along the curve generates the position as  $\mathbf{p}(X) = \int_0^X \mathbf{R}(s)\mathbf{e}_1 ds$ . In general, it is always possible to use  $\Theta(X)$ , that is a coordinate-free parametrization. However, when there is coupling between the rotation matrix and the position vector, one can use an alternative parametrization of the backbone curve by expanding rates of rotation

449 parameters such as Euler angles. In the planar case, they reduce to the same  
 450 parametrization.

451 The matrix  $\Theta(X)$  has embedded in it information about instantaneous  
 452 rotational and translational changes as a function of arclength. These can  
 453 be extracted to form a vector  $\mathbf{q}_{\text{sb}} = [v \ \omega]^T$ , where now  $v$  and  $\omega$  are lin-  
 454 ear and angular velocity with respect to arclength  $X$  instead of time  $t$  (as in  
 455 section 2.2.2). The vector  $\mathbf{q}_{\text{sb}} = [v \ \omega]^T$  can then be expanded using a modal  
 456 approach, that describes the spatio-temporal behavior of  $v$  and  $\omega$ . This modal  
 457 expansion is commonly defined as  $\mathbf{q}_{\text{sb}}(X, t) = \sum_{i=1}^n \Phi_i(X) a_i(t)$ , where  $\Phi_i(X)$   
 458 are modes describing the spatial behaviour of the system, and  $a_i(t)$  are coeffi-  
 459 cients describing its evolution in time. The  $v$ -part of this vector describes how  
 460 the backbone curve stretches and how adjacent planar sections shear relative  
 461 to each other. The  $\omega$ -part of this vector describes bending and twisting, and  
 462 is related to the classical concepts of curvature and torsion of space curves.  
 463 The modal expansion includes as a special case piecewise-constant curvature  
 464 models by choosing some functions  $\Phi_i(X)$  to be piecewise constant for some  
 465 values of  $X$  and equal to zero for others, as described in [31].

466 The parametrization and modal expansion introduced lead to a set of ordi-  
 467 nary differential equations, that can be written using the formalism introduced  
 468 in equation (1), where

469  $\mathcal{D}$  becomes  $d/dt$ , the total derivative with respect to time  $t$ ,

470  $\hat{\mathbf{q}}_{\text{sb}}$  becomes  $[v \ \omega]^T$ , and

471  $\mathcal{N}$  becomes  $-1/\mathbf{M} [\mathbf{D}(\mathbf{s}_{\text{sb}}, \mathbf{q}_{\text{sb}}) + \mathbf{K}(\mathbf{s}_{\text{sb}})]$ , where  $\mathbf{s}_{\text{sb}}$  is the displacement of the  
 472 soft body.

473 The nonlinear term just introduced is derived from the robot dynamic model,  
 474 where  $\mathbf{M}$  is the inertial matrix,  $\mathbf{D}$  is a dissipative term that includes internal  
 475 friction and other dissipative forces (such as Coriolis forces), and  $\mathbf{K}$  is an elastic  
 476 term that encapsulate the stiffness of the system.

477 The coupling with actuation is achieved via an appropriate choice of the  
 478 modal expansion, and it is commonly represented via  $\mathcal{C}_{\text{int}} = \boldsymbol{\alpha}$ , where  $\boldsymbol{\alpha}$  is  
 479 the vector of actuation forces. When motors specify the angles between rigid  
 480 links of a traditional robot, the modes would be Dirac delta functions in  $\omega$  to  
 481 describe revolute joints or in  $v$  to describe prismatic joints, and the weights  
 482 would be the joint angles, and the actuation forces would be joint torques. In  
 483 this sense, the modal approach can be used not only for soft/continuum robots  
 484 but also for ones composed of rigid links, as well as hybrids.

485 The solution of the models in sections 2.2.1 and 2.2.2 requires the use  
 486 of numerical methods, e.g., finite and spectral element approximations. In  
 487 contrast, solution methods for the ordinary differential equations arising in  
 488 this section are based on iterative schemes that update the weights  $a_i(t)$  in  
 489 time. These involve inverse Jacobian iterations as described in [30–32].

490 The computational benefit of this approach is that instead of solving partial  
 491 differential equations, it averages properties over each section and reduces the  
 492 problem to a finite number of ordinary differential equations. This approach

493 has been applied to hyper-redundant manipulators of all kinds (i.e., those  
494 consisting of a large number of rigid links, continuum filament, soft) over the  
495 past several decades. Successful implementation in the realm of soft robotics  
496 applications exist, see for instance [33, 34].

#### 497 *2.2.4 Data-driven and machine learning models*

498 An alternative approach to the models above is the use of machine learn-  
499 ing techniques. In robotics, learning has been widely used for building the  
500 kinematic and dynamic relations between a robot actuators and its position  
501 in space. Neural networks have been used to this aim, mainly for control  
502 purposes, implementing so-called neuro-controllers. In the same way, in soft  
503 robots, neural networks can be used to learn the soft body dynamics and solve  
504 the transformations from the actuator space to the space of the soft body  
505 deformation and position. Following the formalism in equation (1), one tries  
506 to learn the nonlinear and the coupling term for internal interactions,  $\mathcal{N}$  and  
507  $\mathcal{C}_{\text{int}}$ . This results in learning the right-hand side of equation (1) in one go, with  
508 e.g., a neural network (NN):  $\mathcal{D}\mathbf{q}_{\text{sb}} = \text{NN}[\mathbf{q}_{\text{sb}}(k) \rightarrow \mathbf{q}_{\text{sb}}(k + 1)]$ , where  $k$  are  
509 different time instances.

510 In [35], an analysis is given of how learning-based blocks can replace some  
511 of the steps of the longer transformation chain involved in soft robot control.  
512 Diverse network topologies and learning paradigms can be used for this  
513 purpose. In [36], a quantitative survey is presented, showing how supervised  
514 learning is more widely used than unsupervised or reinforcement learning,  
515 with references to the different techniques used. The survey presented in  
516 [37] describes the learning techniques used for obtaining the mapping from  
517 actuation space to task space in continuum robots.

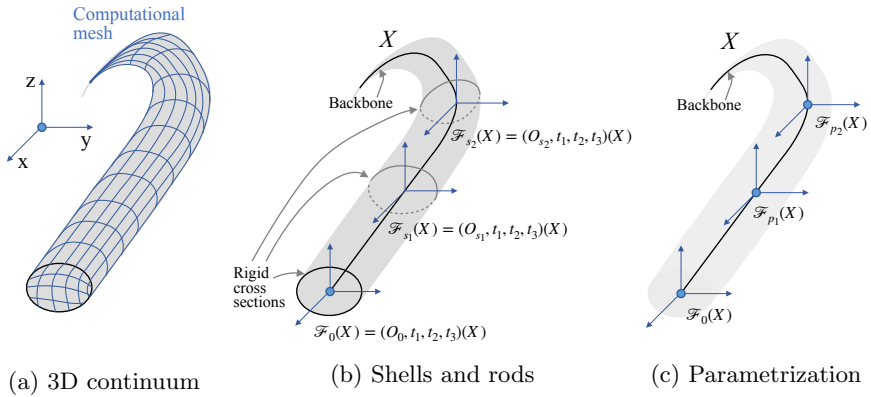
518 An interesting comparison between a model-based and a learning-based  
519 approach to the control of a same soft robot arm is presented in [38]. While the  
520 model-based method is more accurate in controlling the end-effector position,  
521 as resulting in simulation, its error tends to increase together with the model  
522 inaccuracies, e.g., fabrication inaccuracies. The learning-based controller error  
523 tends to be insensitive to such modeling inaccuracies, especially if training is  
524 accomplished on the physical robot arm.

525 Looking ahead, we envisage a promising direction of progress in the inte-  
526 gration of modeling techniques with machine learning, where models can feed  
527 neural networks and learning can replace specific sub-system mappings.

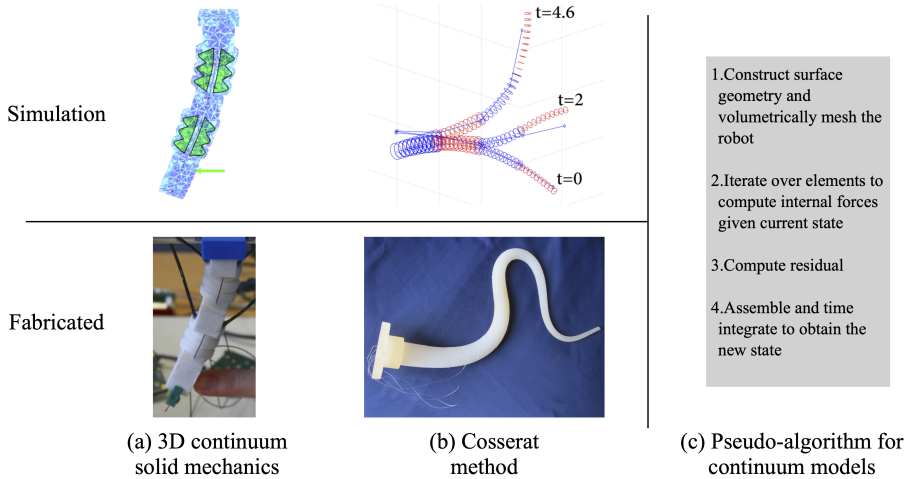
528 More broadly, there is a wealth of literature on data-driven and reduced-  
529 order modeling techniques that may be used to capture challenging aspects of  
530 soft-robot internal interactions, such as the two-way coupling in fluid structure  
531 interactions. System identification [39] may be viewed as a predecessor of many  
532 modern techniques in machine learning, and this field has a rich history going  
533 back at least seven decades [40]. For example, considerable work has gone into  
534 linear system identification, based on frequency-response and impulse-response  
535 data, which is useful for modeling small deflections, especially when feedback  
536 control is used to keep the system in a region where linearization is valid.



537 For large-amplitude motions and unsteadiness, nonlinear model reduction and  
 538 system identification have become mature techniques [41–45].



**Fig. 3:** A conceptual illustration of the models for internal interactions described in section 2, applied to the octopus arm of Fig. 2. (a) A representation of the mesh description in 3D continuum mechanics models. (b) Cosserat’s approach for rods. (c) Finite-dimensional parametrization models.



**Fig. 4:** Examples of practical simulations in the context of internal interactions achieved via (a) 3D continuum solid mechanics, and (b) Cosserat. The 3D continuum solid mechanics model is solved using SOFA [8], while the Cosserat model is solved using the methodology described in [46]. In both subfigures (a) and (b), we depict the simulation (top) along with the fabricated (bottom) soft body. In the figure, we also present (c) a simplified pseudo-algorithm for internal interactions in the context of continuum models (i.e., 3D continuum solid mechanics and Cosserat method), noting that the specific details depend on the resolution technique adopted.

### 3 External interactions

#### 3.1 Challenges

To benefit from embodied intelligence, we require medium–robot interaction modeling that can grasp the emergence of sensory–motor behaviour from the interplay with the surrounding environment. Modeling these external interactions, and coupling them with the internal interactions discussed in the previous section, closes the gap required to modeling the physics of embodied intelligence.

The task when modeling external interactions is to capture the complex, time-varying forces between the actuated soft-robot structures and the surrounding medium. The dynamics of fluids and deformable solids are generally nonlinear and unsteady, and interactions between the soft robot and the medium may create complex feedback loops and hysteresis effects. The key challenges to modeling external interactions are:

1. the multiphysics nature of the problem, that requires substantial interdisciplinary efforts, and

555 2. the partially known interfacial physics and unmodeled dynamics (e.g.,  
 556 nonlinear friction and turbulent drag).

557 In the following, we focus on medium-robot interaction, that we denote with  
 558 the coupling term  $\mathcal{C}_{\text{ext}}$  introduced in equation (1). Here, the surrounding  
 559 medium is either a fluid or a solid. The robot (i.e. the soft body) is assumed  
 560 to be described by the models presented in section 2, along with its actuation.  
 561 In general, any of the soft-body models in section 2 can be used in conjunction  
 562 with the models introduced next, unless otherwise specified.

## 563 3.2 Fluid models

564 When fluid forces acting on a robot have a tangible impact on movement, as  
 565 with the octopus in Fig. 2, modeling fluid–robot interaction becomes essential.  
 566 Here the task is to capture the complex, time-varying, bidirectional forces  
 567 between the actuated soft robot structures and the surrounding fluid flow. To  
 568 this end, the field of fluid–structure interaction [47] is a key cross-discipline  
 569 that should be taken into account.

570 We describe three main modeling strategies, that can be adopted in the  
 571 context of fluid–robot interaction. These include continuum fluid mechanics  
 572 models, simplified lumped parameter models, and the relatively new field of  
 573 machine learning for flow modeling. We remark that we keep the description  
 574 at a general level, and we avoid entering into details that may hinder grasping  
 575 the essence of these modeling strategies.

### 576 3.2.1 Continuum fluid mechanics models

In analogy to continuum solid mechanics, the equations governing flow physics  
 in a continuum setting can be considered as the most general model of a  
 fluid interacting with the soft body described in section 2 (see Fig. 5(a)).  
 The equations describing continuum fluid mechanics are the Navier-Stokes  
 equations, constituted, in the most general case, by conservation of mass,  
 momentum and energy. From a soft robot perspective, the action of the fluid  
 modeled by the Navier-Stokes equations emerges in the form of equality con-  
 straints at the interface between the soft body and the fluid, denoted by  $\Gamma_{\text{sb},f}$ .  
 In particular, we can write these interface constraints as follows:

$$\mathcal{I}_{e,f} = \begin{cases} \mathbf{q}_{\text{sb}} = \mathbf{q}_{\text{f}} & \text{on } \Gamma_{\text{sb},f} & (2a) \\ \boldsymbol{\sigma}_{\text{sb}} \cdot \mathbf{n} = \boldsymbol{\sigma}_{\text{f}} \cdot \mathbf{n} & \text{on } \Gamma_{\text{sb},f} & (2b) \\ \mathbf{x}_{\text{sb}} = \mathbf{x}_{\text{f}} & \text{on } \Gamma_{\text{sb},f}. & (2c) \end{cases}$$

577 In equation (2),  $\mathbf{q}_{\text{sb}} = \mathbf{v}_{\text{sb}}$  corresponds to the velocity of the soft body,  
 578 and  $\mathbf{q}_{\text{f}} = \mathbf{v}_{\text{f}}$  is the velocity of the fluid at the interface  $\Gamma_{\text{sb},f}$ ,  $\mathbf{n}$  is the normal  
 579 at any soft body location,  $\boldsymbol{\sigma}_{\text{f}}$  is the fluid Cauchy stress tensor composed of  
 580 the sum of the deviatoric stress tensor  $\boldsymbol{\tau}^{(f)}$  (that accounts for the viscosity)  
 581 and a pressure term  $-p\mathbf{I}$ , and  $\mathbf{x}_{\text{sb}}$  and  $\mathbf{x}_{\text{f}}$  are the positions of the soft body

582 and fluid interfaces, respectively. The solution for the solid velocity is achieved  
583 through the modeling strategies introduced in section 2. The solution for the  
584 fluid velocity is instead obtained by solving the Navier-Stokes equations. For  
585 the purpose of this article, we report the momentum equation, that can be  
586 written as follows:  $\partial(\rho_f \mathbf{q}_f)/\partial t + \nabla \cdot (\rho_f \mathbf{q}_f \otimes \mathbf{q}_f) = \nabla \cdot \boldsymbol{\sigma}_f + \boldsymbol{\beta}_f$ , where  $\rho_f$  is  
587 the fluid density, and  $\boldsymbol{\beta}_f$  is a forcing term acting on the fluid (e.g., gravity).  
588 Depending on the nature of the problem, we can have several approximations,  
589 including incompressible Navier-Stokes equations, where the density is a constant,  
590 compressible Navier-Stokes equations, where the density is not constant  
591 and the flow might develop shock waves, thin-layer Navier-Stokes equations,  
592 that describes flow in thin layers, and potential flow equations that describe  
593 irrotational flows, to cite a few.

594 The compatibility conditions in equation (2) can enter into the equations  
595 describing the soft body (1) as Lagrange multipliers  $\mathcal{C}_{\text{ext}} = \boldsymbol{\Lambda}^T \mathcal{I}_{\text{e,f}}$ , or being  
596 imposed as external equality constraints  $\mathcal{I}_{\text{e,f}}$  or as boundary conditions. Given  
597 the nature of the coupling, the majority of the soft body models presented in  
598 section 2 may be used, with the due approximations required for coupling. For  
599 instance, in the case of continuum solid mechanics (section 2.2.1), the compatibility  
600 conditions are applied to the interface nodes between the soft body  
601 mesh and the fluid mesh (or a proxy representing the interface, if the soft  
602 body / fluid nodes are not matching). In this case, there exist two mainstream  
603 approaches for coupling: partitioned and monolithic. The former uses a structural  
604 and a fluid solver iteratively until convergence, while the latter solves a  
605 fully coupled system of equations in one go [48]. When using continuum fluid  
606 mechanics in conjunction with simplified methods, such as finite-dimensional  
607 parametrization models (section 2.2.3), one instead needs to lump the effect  
608 of the fluid solution into a set of degrees of freedom compatible with the finite  
609 expansions used to describe the deformation of the body.

610 In terms of solution strategies, there exist well-established approaches in  
611 the realm of fluid–structure interaction methods. The two main approaches  
612 are conforming and non-conforming methods [48]. The former enforces  
613 equations (2b) and (2c), while the latter enforces equation (2a). Conforming  
614 methods can be used in conjunction with partitioned methods, where a  
615 popular algorithm is the arbitrary Lagrangian Eulerian approach [49]. Non-  
616 conforming methods are typically used with monolithic methods, where a  
617 popular algorithm is the immersed boundary method [50–52].

618 Continuum fluid mechanics and its interaction with soft bodies have been  
619 investigated in biology [53, 54]. Yet, muscular activation and its full coupling  
620 with the fluid is still problematic. This issue is also present for soft robots,  
621 where muscular activation is replaced by the actuation strategies introduced in  
622 section 2.1. For instance, in the case of fluidic actuation, it is necessary to consider  
623 both the coupling of the external and of the internal fluid with the soft  
624 body. It is exactly this aspect, namely the accurate coupling of the external  
625 fluid with the soft body dynamics and actuation system, as well as the coupling  
626 of the actuation system with the soft body, that constitute an important

627 modeling challenge in this context. In addition, the demanding computational  
 628 costs further hamper the use of continuum fluid mechanics models.

629 To solve the equations arising in this modeling strategy, there exist both  
 630 commercial and open-source multiphysics packages. These include ANSYS [14]  
 631 and COMSOL [15], Altair [16], Flow3D [55], Adina [56], and OpenFOAM [57],  
 632 to cite a few. However, these are not readily tuned for soft robotics applications.  
 633 For example, implementing actuation strategies in a nonlinear elastic material  
 634 interacting with an external fluid described by the Navier-Stokes equations,  
 635 where both internal and external interactions are fully coupled with the soft  
 636 body, remains challenging.

637 Continuum fluid mechanics can fully capture the effect that a fluid has on a  
 638 soft robot. However, its inherent computational costs make these models pro-  
 639 hibitive to use for practical design and control purposes, and they have found  
 640 limited use in soft robotics, as of today. As computational resources become  
 641 more available and underlying algorithms more efficient, the scope of these  
 642 models will expand and they may be eventually used for design and control  
 643 purposes. Yet, today they can already be adopted for high-fidelity simulations  
 644 that can grasp the complex behaviour of biological and soft robotics systems  
 645 interacting with a fluid, and extract the key physical principles underlying  
 646 their embodied intelligence. These principles can in turn improve simplified  
 647 and less expensive models used for design and control.

### 648 3.2.2 Lumped parameter models

649 In some circumstances, it is acceptable and convenient to simplify the descrip-  
 650 tion of the fluid interacting with the soft body. In these cases, one no longer  
 651 solves the equations governing continuum fluid mechanics, but aggregates  
 652 the overall effect of the fluid into a set of lumped contributions. The main  
 653 lumped contributions consist of added mass, drag/lift forces, and buoyancy  
 654 (see Fig. 5(b)). These can be included as forces into the coupling term  $\mathcal{C}_{\text{ext}}$   
 655 as follows:  $\mathcal{C}_{\text{ext}} = \mathbf{f}_{\text{added mass}} + \mathbf{f}_{\text{drag}} + \mathbf{f}_{\text{lift}} + \mathbf{f}_{\text{buoyancy}}$ , where the subscript  
 656 of each term is self-explanatory. The added mass,  $\mathbf{f}_{\text{added mass}}$ , is the virtual  
 657 mass or inertia added to the soft robot due its need to move the fluid sur-  
 658 rounding it. For instance, if the soft body was a simple sphere immersed  
 659 in an incompressible fluid, the added mass would be equal to  $\mathbf{f}_{\text{added mass}} =$   
 660  $(1/2)\rho_f V_{\text{sb}}[D\mathbf{q}_f/Dt - d\mathbf{q}_{\text{sb}}/dt]$ , where  $D\mathbf{q}_f/Dt$  is the material derivative of the  
 661 fluid velocity,  $d\mathbf{q}_{\text{sb}}/dt$  is the total derivative of the spherical soft body velocity,  
 662  $\rho_f$  is the fluid density and  $V_{\text{sb}}$  is the volume of the spherical soft robot. Drag and  
 663 lift forces are typically proportional to the velocity of the fluid flowing around  
 664 the soft body, and they can be calculated as  $\mathbf{f}_{\text{drag}} = (1/2)\rho_f \mathbf{q}_f A_{\text{sb}} C_{\text{drag}}$ , and  
 665  $\mathbf{f}_{\text{lift}} = (1/2)\rho_f \mathbf{q}_f A_{\text{sb}} C_{\text{lift}}$ , where  $A_{\text{sb}}$  is the area of the soft body exposed to the  
 666 fluid, and  $C_{\text{drag}}$  and  $C_{\text{lift}}$  are the drag and lift coefficients that, for simplified  
 667 geometries, are commonly tabulated. Finally, the buoyancy term is typically  
 668 accounted for as a net vertical force composed by buoyancy plus gravity.

669 The term  $\mathcal{C}_{\text{ext}}$  just defined enters into the right-hand side of the soft-body  
 670 equation (1) as a forcing term, and can be used in conjunction with any of the

671 models presented in section 2. Obviously, the lumped contributions need to  
672 correctly interface with the degrees of freedom of the soft body. In the case of  
673 continuum solid mechanics models, (i.e., the ones introduced in sections 2.2.1  
674 and 2.2.2), the lumped forces need to be distributed onto the nodes under-  
675 lying the discretization of the soft body. Similarly, for finite-dimensional  
676 parametrization models (i.e., the ones introduced in section 2.2.3),  $\mathcal{C}_{\text{ext}}$  needs  
677 to be applied to the degrees of freedom of the functional parametrization  
678 adopted.

679 The coupling term  $\mathcal{C}_{\text{ext}}$ , and its constitutive components, (i.e., added mass,  
680 lift, drag and buoyancy) depend on the shape of the soft body, and therefore  
681 they can change over time as effect of actuations or interactions with the envi-  
682 ronment. Employing such changes to increase efficiency, to direct behaviours,  
683 or to improve performances is key to establish quantitative advantages of soft  
684 robotics.

685 In practice, the forces expressed in  $\mathcal{C}_{\text{ext}}$  are often coupled with contin-  
686 uum solid models of soft robots (i.e., the ones described in section 2.2.1 and  
687 2.2.2), such that a complete coupling between continuum fluid mechanics mod-  
688 els and continuum solid mechanical models is generally not performed due to  
689 its computational costs. Successful implementation of these strategies in soft  
690 robotics has been performed, for example in [58] and [46]. In Fig. 6-(a), we  
691 show an example of lumped-parameter model for fluid-solid interaction, used  
692 for simulating a flagellate [46].

693 Eventually, even if external forces are included without modelling the con-  
694 tinuum of the fluid, the dependence of such forces on shape-varying coefficients  
695 allows reaching a trade-off between accuracy and relevance of simulation, with  
696 the computational power available for modelling. Depending on the goal of  
697 the simulation, this is similar to fluid-structure interaction in the aerospace  
698 industry: while complete coupled simulations are used for design, flight simu-  
699 lators employ a similar coupling to match fidelity of simulation with real-time  
700 computation.

### 701 *3.2.3 Data-driven and machine learning models*

702 Recent data-driven and machine learning methods have become widely used  
703 for modeling complex fluids [59–61]. Several recent approaches have leveraged  
704 machine learning to direct speed up high-fidelity simulation of the Navier-  
705 Stokes equations, especially the ones involving turbulence [62–65]. Indeed, for  
706 complex flows, it is often impractical to resolve all scales of the flow, and  
707 instead researchers employ turbulence models, such as the Reynolds aver-  
708 aged Navier-Stokes (RANS) equations or large eddy simulation (LES). These  
709 approximate the smaller scales, and allow for less computationally expensive  
710 simulations of the Navier-Stokes equations. Machine learning is rapidly advanc-  
711 ing these computational fields [59], providing enhanced data-driven turbulence  
712 closures [66–70]. For even further reduction in computation, it is often possible  
713 to develop reduced-order models (ROMs) that are tailored to a specific flow

714 and provide an optimal balance between accuracy and efficiency. Reduced-  
715 order models are typically at least partially data-driven, as they are based on  
716 modal decompositions [71], and they have close connections to machine learn-  
717 ing. Several recent approaches have provided more accurate and generalizable  
718 ROMs, for example based on sparse regression [43, 44, 72–74], operator infer-  
719 ence [42, 45], and the use of deep neural networks to learn effective coordinate  
720 systems [75]. Other promising recent techniques for physics computation based  
721 on machine learning include physics-informed neural networks [76] and deep  
722 operator networks [77].

723 In addition to using machine learning techniques to develop surrogate  
724 models for the complex fluid environment, there is also a need to model dis-  
725 crepancies that arise in complex multiphysics applications. The equations of  
726 a simple fluid are relatively well understood, but interfacial dynamics, non-  
727 Newtonian fluids, and multiphase flows all pose significant modeling challenges  
728 even to represent the fundamental physical effects in a full-fidelity model, let  
729 alone in a reduced-order model. There are considerable efforts to use machine  
730 learning approaches to model these discrepancies between observed data and  
731 idealized physical models. More generally, machine learning is complementing  
732 the mature fields of system identification and reduced-order modelling [41–45],  
733 where there are a host of modeling techniques ranging from rather opaque (i.e.,  
734 black box) to transparent (i.e., white box). There have been several recent  
735 efforts to augment physics-based approaches with machine learning to model  
736 the discrepancy between the physics model and observed data; this is often  
737 referred to as *residual* learning and has been used to model fluid effects in  
738 flying robots [78].

### 739 3.3 Solid models

740 A model of solid–robot interaction should accurately capture how normal  
741 forces, tangential forces or friction, and adhesion/cohesion forces affect and  
742 can therefore be leveraged by the soft body. To this end, contact mechan-  
743 ics [79] and tribology [80] represent the key broad cross-disciplines for modeling  
744 solid–robot interaction, where modeling the microstructure, e.g., roughness  
745 and topography, can be of crucial importance for tasks like gripping [81].

746 In the following, we outline the main modeling strategies that can be  
747 adopted in the context of solid–robot interaction. These include the use of  
748 continuum solid mechanics to model a deformable solid, simplified lumped  
749 parameter models, and more recent machine learning strategies. A key for these  
750 models to be accurate is related to the frictional interaction, and consequent  
751 constraints at the interface between the solid and the soft robot.

#### 752 3.3.1 Continuum three-dimensional solid mechanics models

753 The models underlying continuum solid mechanics have been introduced in  
754 section 2.2.1, albeit for the soft robot. These models can be used also to  
755 describe a surrounding deformable solid medium (see Fig. 5(c)). Its interac-  
756 tion with the soft robot is described by the coupling term  $\mathcal{C}_{\text{ext}}$  introduced in

757 equation (1). This is typically the result of a series of constraints that need to  
 758 be satisfied at the interface between the soft robot and the solid medium. Such  
 759 constraints are similar to the one introduced in section 3.2.1, except that they  
 760 need to account for complementarities, that is, when the system transition  
 761 from no contact to contact, or from static friction (i.e., no tangential rela-  
 762 tive movement between two elastic surfaces) to dynamic friction (i.e., relative  
 763 tangential movement).

764 For instance, the normal contact between two elastic surfaces can be mod-  
 765 eled using the Signorini’s framework, that uses a distance function  $S_n$  to  
 766 measure the distance between two surfaces along the normal direction. Sig-  
 767 norini’s formulation can be written as  $S_n(\mathbf{q}) \perp \boldsymbol{\sigma}_n$ , where  $\boldsymbol{\sigma}_n$  is the stress along  
 768 the normal direction  $\mathbf{n}$  at the contact interface, and the symbol  $\perp$  denotes com-  
 769 plementarity: if  $S_n(\mathbf{q}) > 0$  then  $\boldsymbol{\sigma}_n = 0$  (no contact); if  $S_n(\mathbf{q}) = 0$  then  $\boldsymbol{\sigma}_n > 0$   
 770 (contact). Tangential or frictional contact can instead be modeled using the  
 771 Coulomb’s law framework, where the complementarity is given by the relation  
 772  $\boldsymbol{\sigma}_t = \mu_s \boldsymbol{\sigma}_n$ . Here, complementarity arises from static vs. dynamic friction. For  
 773  $\boldsymbol{\sigma}_t \leq \boldsymbol{\sigma}_{\max}$  there is static friction (no relative sliding of the two surfaces), while  
 774 for  $\boldsymbol{\sigma}_t > \boldsymbol{\sigma}_{\max}$  there is dynamic friction (relative sliding of the two surfaces),  
 775 where  $\boldsymbol{\sigma}_{\max}$  is the maximum value of stress that allow static friction.

776 These interface conditions need to be encapsulated into the continuum  
 777 solid mechanics models describing the soft robot and the elastic solid medium  
 778 interacting with the robot, in a similar manner as described in section 3.2.1,  
 779 for the constraints in equation (2). They can for instance be embedded into  
 780 the equations through the term  $\mathcal{C}_{\text{ext}} = \mathcal{I}_{e,s} \boldsymbol{\Lambda}$ , using Lagrange multipliers for  
 781 the constraints. However, in contrast to section 3.2.1, one needs to account for  
 782 the complementarities in the contact and friction laws. These complementar-  
 783 ities create jumps in velocities. When the coupled system transitions from one  
 784 regime to another (e.g., from no contact to contact, or from static to dynamic  
 785 friction), the inertial terms underlying the system of equations is not defined.

786 In order to solve this contact problem, it is necessary to rely on numerical  
 787 methods that account for these complementarities, and the singularities they  
 788 produce. To this end, a strategy is first to calculate  $S_n(\mathbf{q})$  using a measurement  
 789 of proximity distance, interpenetration distance, interpenetration volumes, or a  
 790 precise measurement of the moment and the contact configuration between two  
 791 simulation steps. Following this detection, a set of constraints are defined, often  
 792 on contact points (but one can extend to volumes or to non-planar surfaces).  
 793 Finally, the solution can be obtained with different numerical strategies such as  
 794 Lagrange multipliers, penalty methods and augmented Lagrangian methods, in  
 795 conjunction with optimization solvers dedicated to complementarity problems.  
 796 The time-integration of the resulting equations is achieved via event-driven  
 797 or time-stepping methods that account for the singularity in the underlying  
 798 equations – see e.g., [82], [83].

799 An example of successful implementation of this strategy can be found  
 800 in [84]. Here, the contact problem is formulated to solve an inverse model for



801 the control of a soft robot, which leads to writing a quadratic problem with  
 802 complementarity constraints (also referred to as QPCC).

803 Most of the major multiphysics computational software previously cited,  
 804 including ABAQUS [13], ANSYS [14] and COMSOL [15], can be used to solve  
 805 contact between two elastic solids, yet they are not necessarily tailored to  
 806 soft robotics applications. In the article [85], a literature review of physical  
 807 engines for simulation in robotic applications is listed, most of these engines  
 808 support contact modeling. On the other hand, not all engines are adapted to  
 809 deformable robots, in particular to simulate volume deformations. We note the  
 810 SOFA software [86], originally dedicated to medical simulation, offers plug-ins  
 811 dedicated to soft robotics and proposes implementations of FEM and Cosserat  
 812 rods that are compatible with contact modeling. [An example of these capa-](#)  
 813 [bilities is depicted in Fig. 6-\(b\), where SOFA simulates a finger touching a](#)  
 814 [deformable solid.](#)

815 Similar considerations as for continuum fluid mechanics can be made. In  
 816 particular, these models are computationally expensive, and they may lead  
 817 to impractical solutions for soft robotics applications today, especially in the  
 818 context of real-time control.

### 819 3.3.2 Lumped parameter models

820 Similarly to what we have introduced for fluid models, we can consider a  
 821 simplified approach, where we can aggregate the effect of contact between  
 822 two surfaces into lumped contributions. For instance, when the external solid  
 823 can be considered rigid, one can introduce some simplifications to the model  
 824 outlined in section 3.3.1. In particular, the state  $\mathbf{q}_s$  of a rigid body can be rep-  
 825 resented by the position of its center of mass, its orientation, and its linear and  
 826 angular velocity (see Fig. 5(d)). Once these are known, it is possible to formu-  
 827 late the rigid-robot interaction problem. This implies identifying the point of  
 828 contact between the soft body and the rigid solid, and applying an equivalent  
 829 frictional force  $\mathbf{f}$  and torque  $\boldsymbol{\tau}$ , induced by the interaction between the soft  
 830 and the rigid body. The interaction surface between the rigid solid and the  
 831 soft robot is typically modeled as a planar surface. This leads to models that  
 832 contain only the three degrees of freedom associated to frictional forces at the  
 833 planar surface,  $\mathbf{f}$ .

834 In practice, a soft robot interacting with a rigid body leads to non-planar  
 835 contact surfaces, with multiple points of contact. This introduces three addi-  
 836 tional degrees of freedom, and provide a six-dimensional model for the normal  
 837 and frictional wrenches, as both force  $\mathbf{f}$  and torque  $\boldsymbol{\tau}$  are three-dimensional.  
 838 Following the formalism adopted in [87], one can define the normal force  
 839 and torque as  $\mathbf{f}_n = -\int_S p \cdot \mathbf{n} dS$ , and  $\boldsymbol{\tau}_n = -\int_S p \cdot [(\mathbf{r} \times \mathbf{n})] dS$ , respec-  
 840 tively, and the frictional force and torque as  $\mathbf{f}_t = -\mu \int_S p \cdot \mathbf{v}_r dS$ , and  
 841  $\boldsymbol{\tau}_t = -\mu \int_S p \cdot [\mathbf{r} \times \mathbf{v}_r] dS$ , respectively, where  $S$  is the contact surface,  $\mathbf{v}_r$  is the  
 842 relative velocity between the rigid solid and the soft robot,  $\mathbf{n}$  is the normal to  
 843 the contact surface,  $\mathbf{r}$  is the torque arm,  $p$  is the contact pressure distribution,  
 844 and  $\mu$  is the friction coefficient.

845 The coupling is achieved by encapsulating these forces and torques into the  
846 coupling term  $\mathcal{C}_{\text{ext}}$ . This acts as a forcing term on the right-hand side of the  
847 soft body equation, that is  $\mathcal{C}_{\text{ext}} = \mathbf{f}_n + \boldsymbol{\tau}_n + \mathbf{f}_t + \boldsymbol{\tau}_t$ .

848 The computational costs associated with these models are relatively small  
849 compared to the interaction between two deformable solids.

850 Applications of this modeling strategies in soft robotics exists, both in  
851 terms of analytical approaches [88, 89] and computational models [8, 90, 91],  
852 that focused on simulating contact behaviours of soft robot grasping and  
853 manipulation as well as crawling [92, 93]. Inverse model of soft robot in sit-  
854 uation of frictionless contact [84] and adhesive contact situations has been  
855 investigated for control of manipulation and locomotion [94].

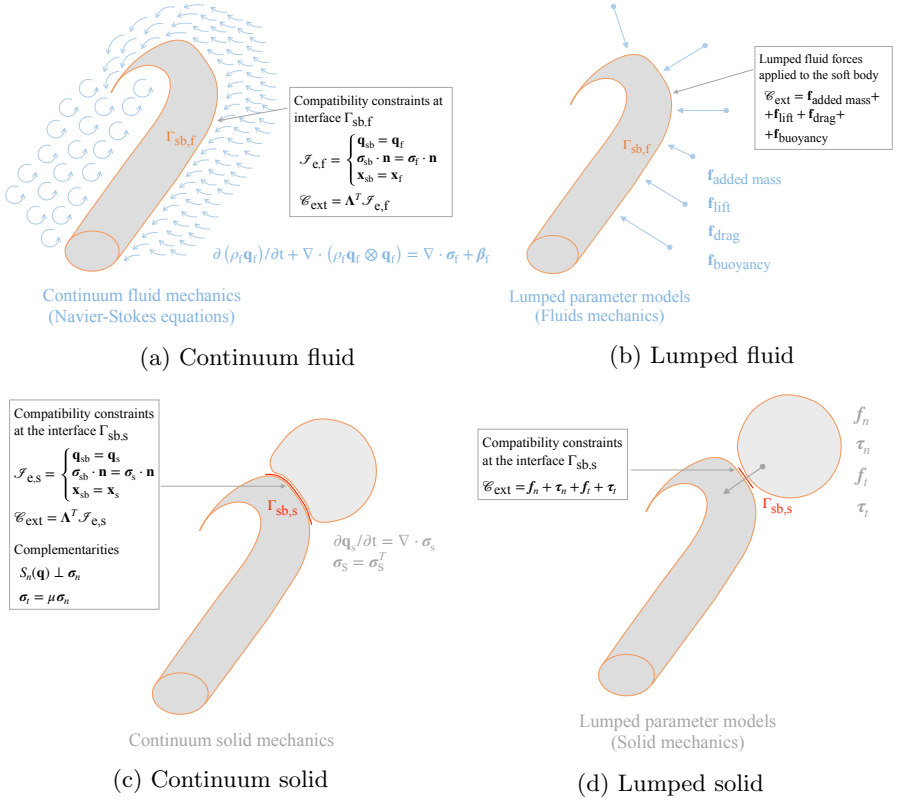
856 These models can be broadly applied for describing several tasks involv-  
857 ing the interaction of the soft robot with e.g., rigid solids, and similar  
858 considerations as in section 3.2.2 can be made.

### 859 3.3.3 *Data-driven and machine learning models*

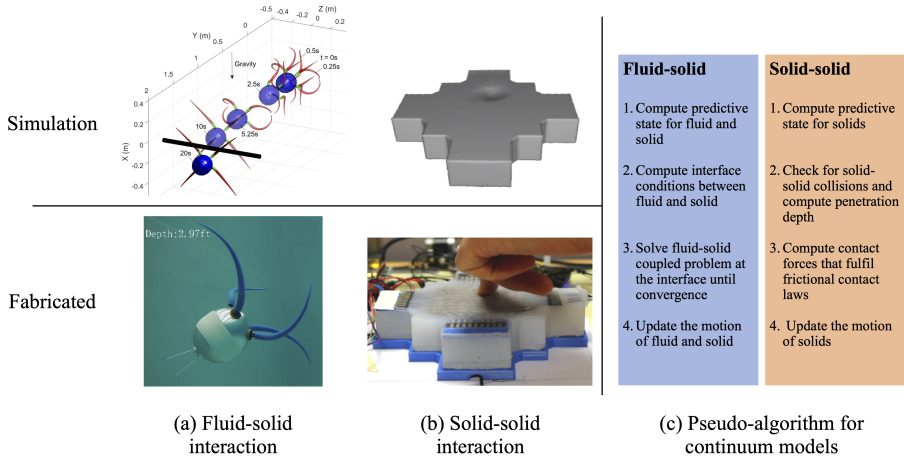
860 Frictional and normal contact modeling is notoriously difficult, and a high  
861 prediction accuracy is onerous to achieve, especially for soft-bodied robots that  
862 interact with environments or objects with vastly different surface properties.  
863 [Within this context machine learning and data-driven approaches have found](#)  
864 [limited use thus far, with few exceptions.](#)

865 Recent efforts explore the augmentation of simulation representations with  
866 neural networks to close sim-to-real gaps (see, e.g., [95–99]). [These efforts](#)  
867 [attempt to](#) reduce the uncertainty that contact with unknown objects or envi-  
868 ronments introduces. A naive approach is to learn the mapping of the previous  
869 to the next state directly. This would mean that the nonlinear equations  $\mathcal{N}$   
870 in equation (1), and also the actuation and [solid-solid interaction](#) constraint  
871 force terms, are replaced with a neural network.

872 However, this is all but practical for complex robots, and it is best to  
873 acquire data for interactions, such as frictional contact, that lead to predic-  
874 tion inaccuracies in our state-of-the-art models, and to only learn corrections.  
875 More specifically, we could learn corrections for the frictional forces that act  
876 on the soft-body, improving a first-order estimate that we get from a known  
877 simulation representation.



**Fig. 5:** A conceptual illustration of the models for external interactions described in section 3, applied to the octopus arm of Fig. 2. (a) Continuum fluid mechanics models. (b) Lumped fluid models. (c) Continuum solid mechanics models. (d) Lumped solid models.



**Fig. 6:** Examples of practical simulations in the context of external interactions for (a) fluid-solid interaction using a lumped-parameter model and for (b) solid-solid interaction using 3D continuum mechanics. The details of the fluid-solid interaction simulation are described in [46], while the solid-solid interaction simulation has been solved using SOFA [8]. In both subfigures (a) and (b), we depict the simulation along with the fabricated soft body. In the figure, we also present (c) a simplified pseudo-algorithm for fluid-solid and solid-solid interactions in the context of continuum mechanics models (i.e., 3D continuum fluid and solid mechanics), noting that the specific details depend on the resolution technique adopted.

## 878 4 From models to practice

879 As emerging from the previous sections, presenting the models involved in  
 880 describing soft robots and embodied intelligence inside a unified framework  
 881 is challenging, yet helpful. Therefore, it is not surprising that a structured  
 882 modeling framework for the physics of interactions in soft robotics remains  
 883 elusive.

884 The models presented range from high-dimensional (sections 2.2.1, 2.2.2  
 885 for internal interactions, and sections 3.3.1, 3.2.1 for external interactions)  
 886 to low-dimensional (section 2.2.3 for internal interactions, and sections 3.3.2,  
 887 3.2.2 for external interactions). The former have found relatively little use in  
 888 soft robotics, due to their computational costs, hence limited applicability for  
 889 control and design purposes. The latter have been instead used with different  
 890 degrees of success due to their simplifications, that may be unable to capture  
 891 the rich physics of internal and external interactions.

892 High-dimensional models can provide a framework for simulation of inter-  
 893 nal and external interactions. Embodied intelligence shifts the challenges of  
 894 realizing a specific task from the control algorithm to such interactions, and

895 therefore to the design stage. The models presented could be employed to  
896 investigate the optimal design to achieve a specific task with minimal feedback  
897 control strategies, or open-loop ones. As an example, in case of manipulation,  
898 diverse designs could be investigated to obtain effective grasping on a variety  
899 of objects by employing the same basic low-level control strategy (by inflating  
900 a pneumatic chamber, or pulling a tendon). It is worth to mention that embodied  
901 intelligence points toward the *effective* expression of a certain behavior,  
902 and not to the *accurate* expression of it. That is, the fingers of a soft gripper  
903 are free to adapt to external interactions up to the point that the grasp  
904 is still stable, and no control actions are expected to place a specific finger in  
905 a specific position. Although most of the time this characteristic is obtained  
906 by physical prototyping and testing a mock-up (“trial-and-error” approach),  
907 it can also be obtained with the high-dimensional models presented, with the  
908 further benefit of including stochastic disturbances to the actuation, materials  
909 or interaction. The embodied intelligence principles allow the design of robust  
910 agents that express the desired behavior in presence of disturbances, and therefore  
911 the sim-to-real gap can be reduced by looking for such robust designs.  
912 These simulations, in turn, can be used to understand the principles behind  
913 an observed and/or desired behaviour and may eventually be adopted for  
914 automatic design [92, 93, 100] in the future, if computational power and algorithms  
915 will allow for a sufficiently fast model-driven workflow. Yet, having these  
916 models permits constructing improved approximated and low-dimensional representations  
917 of soft robots, that capture their overall behaviour at a cheaper  
918 computational cost, feasible for design and control purposes today. Indeed,  
919 the high-dimensional models can capture the key components underpinning  
920 embodied intelligence physical principles, thereby allowing for a more accurate  
921 low-dimensional description of how soft robots can achieve the embodied intelligence  
922 of biological systems. As an example, Fig. 2 depicts a low-dimensional  
923 model for octopus’ underwater locomotion [101]. A low-dimensional description  
924 is typically constituted by a representation of the behaviour of the system  
925 in a reduced space, composed by much fewer degrees of freedom than the  
926 original high-dimensional counterpart [9, 102]. Therefore, one must identify a  
927 suitable low-dimensional representation that retains a sufficient accuracy to  
928 describe the whole system.

929 The discovery of low-dimensional representation (often referred to as fundamental  
930 or parsimonious models) is currently done empirically by observing  
931 the system. Whether a high-dimensional model is available, the synthesis to  
932 the lower-level counterpart (if any) can be obtained more systematically. Accurately  
933 informed fundamental models can capture the overall behaviour of the  
934 soft robot and expose a few key aggregate physical parameters to describe  
935 a specific task (e.g., locomotion, arm movements, etc.). These fundamental  
936 models provide a generic base upon which specific morphology/control could  
937 be developed, following the template/anchor approach proposed in [103]. The  
938 analysis of the fundamental models might increase the comprehension of the  
939 system and expose quantitative advantages of compliant robots over rigid ones.

940 This concept was successfully employed in underwater legged robots, where  
941 shape-dependent forces, elastic leg elements, and pushing-based actuation  
942 interweave to shape the basin of attraction of the hopping limit cycle. Shape  
943 morphing proved how deformable bodies can be exploited to overcome actu-  
944 ation limits [104]. Another remarkable example is presented in [105], where  
945 the elastic components of a soft robotic squid have been exploited to increase  
946 swimming efficiency. A second-order forced oscillation model was developed to  
947 catch the relationship between internal and external forces, mediated by actu-  
948 ation frequency, in an approximate and simplified way. In both cases, they are  
949 not a low-level counterpart of the models presented in section 2 and 3, but  
950 they are fundamental models which capture the specific behavior of interest,  
951 and can provide insights into the design of actual soft robots.

952 All three of the main types of internal and external interactions with fluid  
953 and solid media may benefit from recent advances in machine learning for mod-  
954 eling dynamical systems [60, 62, 63]. However, it is important to understand  
955 the considerable open challenges associated with using machine learning mod-  
956 els for design, optimization, and control. Many machine learning algorithms,  
957 such as deep learning, suffer from limited interpretability and generalizability.  
958 Although they can capture patterns in training data, the resulting models are  
959 often inscrutable and may have limited ability to model new scenarios that  
960 are not captured in the training data. For applications in image classification  
961 and natural language translation, training data is extensive and many plau-  
962 sible uses of a machine learning model may be considered as interpolatory in  
963 nature. In contrast, when using machine learning to accelerate the design of a  
964 new physical system, such as a soft robot, the model must be able to gener-  
965 alize, or *extrapolate*, to new regimes that have not been characterized in the  
966 training data, otherwise a model would not be needed. This capability is par-  
967 ticularly important for inverse-based design optimization, where it is necessary  
968 to model the dependence of the system on the parameters it will be optimized  
969 over. Further, when using machine learning models for design optimization, any  
970 computational savings must be balanced against the cost of acquiring training  
971 data, which is often significant. Using machine learning for control is easier to  
972 justify, as model training is considered an *off-line* expense that is justified by  
973 the increased speed and performance of the model in *on-line* use. It is impor-  
974 tant to note that these challenges have been debated for decades, long before  
975 the rise of machine learning, to understand the role of reduced-order models  
976 more generally in design optimization and control.

## 977 5 Conclusions

978 We walked through the quest for modelling soft robots with a focus on how  
979 to describe the physics involved in their embodied intelligence. We argue that  
980 modelling the deformations of a soft robot body under internal actuation forces  
981 and external interaction forces can capture the practical essence of embodied  
982 intelligence. We outlined the mathematical models used for describing such

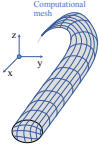
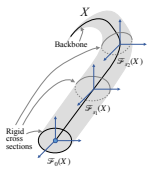
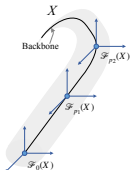
983 internal and external interactions in a soft robot body, including related soft-  
984 ware tools, and we discussed how to use them in practice. For the first time, we  
985 show a unified view of the multiphysics of interactions arising from embodied  
986 intelligence, and we link them to the design of soft robots.

987 Tables 1, and 2 summarize this analysis (not including [data-driven](#) tech-  
988 niques), and provide a practical [and concise guide](#) to the modelling methods  
989 that can be beneficially used in soft robotics , enabling soft robots to fully  
990 leverage on embodied intelligence, acquire unprecedented abilities and respond  
991 to unmet needs, ultimately contributing to further soft robotics progress.

992 We argue that, in contrast to the current trial (physically build the robot)  
993 and error (robot testing) approach, soft-robot design can transition to a  
994 model-informed workflow. Indeed, prototype-driven design (also referred to as  
995 trial-and-error) was likely the fastest and most efficient way to proceed, espe-  
996 cially in the soft robotics exploratory phase. Today, we are at a stage where  
997 computational modelling within a model-driven umbrella can enable (i) scaling  
998 up soft-robot design in response to application needs, (ii) holistic model-based  
999 control embedding external interactions, and (iii) high-fidelity simulations,  
1000 opening the path towards soft-robot digital twins.


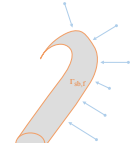
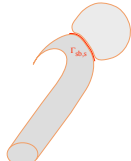
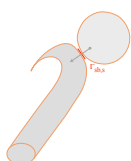
1001 This transition is within grasp, in an interdisciplinary dialogue of roboti-  
1002 cists with communities like computational physics, applied mathematics,  
1003 scientific computing and machine learning. This unified approach will allow soft  
1004 robotics to thrive in the next few decades and establish itself as a model-driven  
1005 scientific discipline that can tangibly impact human activities.

**Table 1:** Summary of models for soft body mechanics and internal interactions, with reference to equation (1). As discussed in Section 2.2.4, machine learning techniques can be also proposed to solve the same modeling problems.

| Model  | $\mathcal{D}$         | $\mathbf{q}_{\text{sb}}$     | $\mathcal{N}_{\text{sb}}$  | $\mathcal{C}_{\text{int}}$   | Software tools  |
|--|-----------------------|------------------------------|--|--|---|
| <p>Continuum 3D solid mechanics</p>  <p>section 2.2.1</p>         | $\partial/\partial t$ | $\mathbf{v}_{\text{sb}}$     | $\nabla \cdot \boldsymbol{\sigma}_{\text{sb}}$   | <p>Actuation imposed as equality and inequality constraints:</p> <p><math>\mathcal{I}_e, \mathcal{I}_i</math>, through <math>\boldsymbol{\Lambda}^T \mathcal{I}_e + \boldsymbol{\Theta}^T \mathcal{I}_i</math> (e.g., Lagrange multipliers)</p> <p>[used with 1D, 2D, 3D actuations]</p> | <p>SOFA [8]<br/>ChainQueen [10]<br/>Evosoro [12]<br/>Voxelyze [11]<br/>ABAQUS [13]<br/>ANSYS [14]<br/>COMSOL [15]<br/>Altair [16]</p> |
| <p>Rods and shells, e.g., Cosserat</p>  <p>section 2.2.2</p>    | $\partial/\partial t$ | $[v, \boldsymbol{\omega}]^T$ | $[\mathcal{N}_{\text{sb},v}, \mathcal{N}_{\text{sb},\boldsymbol{\omega}}]^T$ $\mathcal{N}_{\text{sb},v} = 1/(\rho A)(\partial n/\partial x + \bar{n})$ $\mathcal{N}_{\text{sb},\boldsymbol{\omega}} = I^{-1}/\rho[-\boldsymbol{\omega} \times (\rho I \boldsymbol{\omega}) + \partial c/\partial X + \partial r/\partial X \times \mathbf{n} + \bar{c}]$ | <p>Actuation imposed as active internal wrenches <math>\boldsymbol{\alpha}, \boldsymbol{\tau}</math></p> <p>[used with 1D, 2D actuation]</p>   | <p>SOFA [8]<br/>Elastica [28]<br/>SoRoSim [29]</p>  |
| <p>Finite-dimensional parametrization</p>  <p>section 2.2.3</p> | $d/dt$                | $[v, \boldsymbol{\omega}]^T$ | $-1/\mathbf{M} [\mathbf{D}(\mathbf{s}_{\text{sb}}, \mathbf{q}_{\text{sb}}) + \mathbf{K}(\mathbf{s}_{\text{sb}})]$ <p><math>\mathbf{s}_{\text{sb}}</math> is the displacement of the soft body</p>  | <p>Actuator forces grouped in a vector <math>\boldsymbol{\alpha}</math> that acts as a forcing term on the right-hand side</p> <p>[used with 1D actuation]</p>   | <p>Bespoke tools written in various languages</p>   |



**Table 2:** Summary of models for external interactions, with reference to equation (1). As discussed in sections 3.2.3 and 3.3.3, machine learning techniques can be also proposed to solve the same modeling problems.

| Fluid models  | $\mathcal{C}_{\text{ext}}$   | Software tools   |
|---|--|--|
| Continuum fluid mechanics<br><br>section 3.2.1   | Compatibility constraints at interface $\Gamma_{\text{sb},f}$ :<br>$\mathcal{I}_{e,f} = \begin{cases} \mathbf{q}_{\text{sb}} = \mathbf{q}_f \\ \boldsymbol{\sigma}_{\text{sb}} \cdot \mathbf{n} = \boldsymbol{\sigma}_f \cdot \mathbf{n} \\ \mathbf{x}_{\text{sb}} = \mathbf{x}_f \end{cases}$ $\mathcal{C}_{\text{ext}} = \mathbf{\Lambda}^T \mathcal{I}_{e,f}$ (e.g., Lagrange multipliers)<br>Segregated, monolithic approaches   | ANSYS [14]<br>COMSOL [15]<br>Altair [16]<br>Flow3D [55]<br>Adina [56]<br>OpenFOAM [57] |
| Lumped parameters<br><br>section 3.2.2           | Fluid forces applied on the right-hand side of equation (1) as aggregated contributions<br>$\mathbf{f}_{\text{added mass}} + \mathbf{f}_{\text{drag}} + \mathbf{f}_{\text{lift}} + \mathbf{f}_{\text{buoyancy}}$   | Bespoke tools written in various languages   |
| Solid models  | $\mathcal{C}_{\text{ext}}$   | Software tools   |
| Continuum solid mechanics<br><br>section 3.3.1 | Compatibility constraints at interface $\Gamma_{\text{sb},s}$ :<br>$\mathcal{I}_{e,s} = \begin{cases} \mathbf{q}_{\text{sb}} = \mathbf{q}_s \\ \boldsymbol{\sigma}_{\text{sb}} \cdot \mathbf{n} = \boldsymbol{\sigma}_s \cdot \mathbf{n} \\ \mathbf{x}_{\text{sb}} = \mathbf{x}_s \end{cases}$ $\mathcal{C}_{\text{ext}} = \mathbf{\Lambda}^T \mathcal{I}_{e,s}$ (e.g., Lagrange multipliers)<br>Complementarities<br>$S_n(\mathbf{q}) \perp \boldsymbol{\sigma}_n$<br>$\boldsymbol{\sigma}_t = \mu \boldsymbol{\sigma}_n$ | SOFA [8]<br>ABAQUS [13]<br>ANSYS [14]<br>COMSOL [15]                                   |
| Lumped parameters<br><br>section 3.3.2         | Normal and tangential forces and torques applied on the right-hand side of equation (1) as aggregated contributions<br>$\mathbf{f}_n + \boldsymbol{\tau}_n + \mathbf{f}_t + \boldsymbol{\tau}_t$   | SOFA [8] and other bespoke tools written in various languages                          |

1006 **Acknowledgments** Gianmarco Mengaldo acknowledges NUS support  
1007 through his start-up grant (R-265-000-A36-133). Gregory Chirikjian acknowl-  
1008 edges MOE Tier 1 grant (R-265-000-655-114) . Cecilia Laschi acknowledges  
1009 NUS support through her start-up grant (R-265-000-A31-133 and R-265-  
1010 000-A31-731) .Part of this research is supported by the National Research  
1011 Foundation, Singapore, under its Medium Sized Centre Programme - Centre  
1012 for Advanced Robotics Technology Innovation (CARTIN). Gianmarco Men-  
1013 galdo, Gregory Chirikjian, and Cecilia Laschi acknowledge MOE Tier 2 grant  
1014 ‘REBOT’. This work was supported in part by the Khalifa University of Sci-  
1015 ence and Technology under Grants CIRA-2020-074, RC1-2018-KUCARS, and  
1016 the Office of Naval Research Global under Grant N62909-21-1-2033.

## 1017 **References**

- 1018 [1] Kim, S., Laschi, C., Trimmer, B.: Soft robotics: a bioinspired evolution  
1019 in robotics. *Trends in biotechnology* **31**(5), 287–294 (2013)
- 1020 [2] Pfeifer, R., Lungarella, M., Iida, F.: Self-organization, embodiment, and  
1021 biologically inspired robotics. *science* **318**(5853), 1088–1093 (2007)
- 1022 [3] Blickhan, R., Seyfarth, A., Geyer, H., Grimmer, S., Wagner, H., Günther,  
1023 M.: Intelligence by mechanics. *Philosophical Transactions of the Royal*  
1024 *Society A: Mathematical, Physical and Engineering Sciences* **365**(1850),  
1025 199–220 (2007)
- 1026 [4] Niederer, S.A., Sacks, M.S., Girolami, M., Willcox, K.: Scaling digital  
1027 twins from the artisanal to the industrial. *Nature Computational Science*  
1028 **1**(5), 313–320 (2021)
- 1029 [5] Brunton, S.L., Nathan Kutz, J., Manohar, K., Aravkin, A.Y., Mor-  
1030 gansen, K., Klemisch, J., Goebel, N., Buttrick, J., Poskin, J., Blom-  
1031 Schieber, A.W., Hogan, T., McDonald, D.: Data-driven aerospace engi-  
1032 neering: reframing the industry with machine learning. *AIAA Journal*  
1033 **59**(8), 2820–2847 (2021)
- 1034 [6] Xavier, M.S., Fleming, A.J., Yong, Y.K.: Finite element modeling of  
1035 soft fluidic actuators: Overview and recent developments. *Advanced*  
1036 *Intelligent Systems* **3**(2), 2000187 (2021)
- 1037 [7] Vanneste, F., Goury, O., Duriez, C.: Enabling the control of a new degree  
1038 of freedom by using anisotropic material on a 6-dof parallel soft robot.  
1039 In: *Robosoft 2021* (2021)
- 1040 [8] Duriez, C., Bieze, T.: Soft robot modeling, simulation and control in  
1041 real-time. In: *Soft Robotics: Trends, Applications and Challenges*, pp.  
1042 103–109 (2017)

- 1043 [9] Goury, O., Duriez, C.: Fast, generic, and reliable control and simula-  
1044 tion of soft robots using model order reduction. *IEEE Transactions on*  
1045 *Robotics* **34**(6), 1565–1576 (2018)
- 1046 [10] Hu, Y., Liu, J., Spielberg, A., Tenenbaum, J.B., Freeman, W.T., Wu, J.,  
1047 Rus, D., Matusik, W.: Chainqueen: A real-time differentiable physical  
1048 simulator for soft robotics. In: 2019 International Conference on Robotics  
1049 and Automation (ICRA), pp. 6265–6271 (2019)
- 1050 [11] Hiller, J., Lipson, H.: Dynamic simulation of soft multimaterial 3d-  
1051 printed objects. *Soft robotics* **1**(1), 88–101 (2014)
- 1052 [12] Cheney, N., MacCurdy, R., Clune, J., Lipson, H.: Unshackling evolution:  
1053 evolving soft robots with multiple materials and a powerful generative  
1054 encoding. *ACM SIGEVOlution* **7**(1), 11–23 (2014)
- 1055 [13] ABAQUS software. [https://www.3ds.com/products-services/simulia/  
1056 products/abaqus/](https://www.3ds.com/products-services/simulia/products/abaqus/). Accessed: 2021-10-27
- 1057 [14] ANSYS software. <https://www.ansys.com>. Accessed: 2021-10-27
- 1058 [15] COMSOL software. <https://www.comsol.com>. Accessed: 2021-10-27
- 1059 [16] Altair software. <https://www.altair.com>. Accessed: 2021-10-27
- 1060 [17] Turner, M., Peiró, J., Moxey, D.: Curvilinear mesh generation using a  
1061 variational framework. *Computer-Aided Design* **103**, 73–91 (2018)
- 1062 [18] Mengaldo, G., Moxey, D., Turner, M., Moura, R.C., Jassim, A., Taylor,  
1063 M., Peiro, J., Sherwin, S.J.: Industry-relevant implicit large-eddy simu-  
1064 lation of a high-performance road car via spectral/hp element methods.  
1065 arXiv preprint arXiv:2009.10178 (2020)
- 1066 [19] Cottrell, J.A., Hughes, T.J.R., Bazilevs, Y.: *Isogeometric Analysis:  
1067 Toward Integration of CAD and FEA*
- 1068 [20] Hoshyari, S., Xu, H., Knoop, E., Coros, S., Bächer, M.: Vibration-  
1069 minimizing motion retargeting for robotic characters. *ACM Trans.*  
1070 *Graph.* **38**(4) (2019). <https://doi.org/10.1145/3306346.3323034>
- 1071 [21] Adagolodjo, Y., Renda, F., Duriez, C.: Coupling numerical deformable  
1072 models in global and reduced coordinates for the simulation of the direct  
1073 and the inverse kinematics of soft robots. *IEEE Robotics and Automa-  
1074 tion Letters* **6**(2), 3910–3917 (2021). [https://doi.org/10.1109/LRA.2021.  
1075 3061977](https://doi.org/10.1109/LRA.2021.3061977)
- 1076 [22] Antman, S.: *Nonlinear Problems of Elasticity*. Applied Mathematical  
1077 Sciences. Springer, ??? (2006)

- 1078 [23] Meier, C., Popp, A., Wall, W.A.: Geometrically exact finite element for-  
1079 mulations for slender beams: Kirchhoff–love theory versus simo–reissner  
1080 theory. *Archives of Computational Methods in Engineering* **26**(1),  
1081 163–243 (2019). <https://doi.org/10.1007/s11831-017-9232-5>
- 1082 [24] Shabana, A.A.: Continuum-based geometry/analysis approach for flexi-  
1083 ble and soft robotic systems. *Soft Robotics* **5**(5), 613–621 (2018). <https://doi.org/10.1089/soro.2018.0007>
- 1085 [25] Boyer, F., Lebastard, V., Candelier, F., Renda, F.: Dynamics of contin-  
1086 uum and soft robots: A strain parameterization based approach. *IEEE*  
1087 *Transactions on Robotics* **37**(3), 847–863 (2020)
- 1088 [26] Boyer, F., Renda, F.: Poincaré’s equations for cosserat media: Applica-  
1089 tion to shells. *Journal of Nonlinear Science* **27**(1), 1–44 (2017)
- 1090 [27] Renda, F., Seneviratne, L.: A geometric and unified approach for mod-  
1091 eling soft-rigid multi-body systems with lumped and distributed degrees  
1092 of freedom. In: 2018 IEEE International Conference on Robotics and  
1093 Automation (ICRA), pp. 1567–1574 (2018). [https://doi.org/10.1109/](https://doi.org/10.1109/ICRA.2018.8461186)  
1094 [ICRA.2018.8461186](https://doi.org/10.1109/ICRA.2018.8461186)
- 1095 [28] Gazzola, M., Dudte, L., McCormick, A., Mahadevan, L.: Forward and  
1096 inverse problems in the mechanics of soft filaments. *Royal Society open*  
1097 *science* **5**(6), 171628 (2018). <https://doi.org/10.1098/rsos.171628>
- 1098 [29] Mathew, A.T., Hmida, I.B., Armanini, C., Boyer, F., Renda, F.: Sorosim:  
1099 a matlab toolbox for soft robotics based on the geometric variable-strain  
1100 approach. arXiv preprint arXiv:2107.05494 (2021)
- 1101 [30] Fu, Q., Gart, S.W., Mitchel, T.W., Kim, J.S., Chirikjian, G.S., Li, C.:  
1102 Lateral oscillation and body compliance help snakes and snake robots  
1103 stably traverse large, smooth obstacles. *Integrative and comparative*  
1104 *biology* **60**(1), 171–179 (2020)
- 1105 [31] Chirikjian, G.S., Burdick, J.W.: A modal approach to hyper-redundant  
1106 manipulator kinematics. *IEEE Transactions on Robotics and Automa-*  
1107 *tion* **10**(3), 343–354 (1994)
- 1108 [32] Kim, B., Ha, J., Park, F.C., Dupont, P.E.: Optimizing curvature sensor  
1109 placement for fast, accurate shape sensing of continuum robots. In: 2014  
1110 IEEE International Conference on Robotics and Automation (ICRA),  
1111 pp. 5374–5379 (2014). IEEE
- 1112 [33] Suzumori, K., Iikura, S., Tanaka, H.: Development of flexible microac-  
1113 tuator and its applications to robotic mechanisms. In: Proceedings.  
1114 1991 IEEE International Conference on Robotics and Automation, pp.

- 1115 1622–1623 (1991). IEEE Computer Society
- 1116 [34] Webster III, R.J., Jones, B.A.: Design and kinematic modeling of con-  
1117 stant curvature continuum robots: A review. *The International Journal of*  
1118 *Robotics Research* **29**(13), 1661–1683 (2010)
- 1119 [35] George Thuruthel, T., Ansari, Y., Falotico, E., Laschi, C.: Control strate-  
1120 gies for soft robotic manipulators: A survey. *Soft robotics* **5**(2), 149–163  
1121 (2018)
- 1122 [36] Kim, D., Kim, S.-H., Kim, T., Kang, B.B., Lee, M., Park, W., Ku, S.,  
1123 Kim, D., Kwon, J., Lee, H., *et al.*: Review of machine learning methods  
1124 in soft robotics. *Plos one* **16**(2), 0246102 (2021)
- 1125 [37] Wang, X., Li, Y., Kwok, K.-W.: A survey for machine learning-based  
1126 control of continuum robots. *Frontiers in Robotics and AI*, 280 (2021)
- 1127 [38] Giorelli, M., Renda, F., Calisti, M., Arienti, A., Ferri, G., Laschi, C.:  
1128 Neural network and jacobian method for solving the inverse statics of  
1129 a cable-driven soft arm with nonconstant curvature. *IEEE Transactions*  
1130 *on Robotics* **31**(4), 823–834 (2015)
- 1131 [39] Juang, J.N.: *Applied System Identification*. Prentice Hall PTR, Upper  
1132 Saddle River, New Jersey (1994)
- 1133 [40] Brunton, S.L., Kutz, J.N.: *Data-Driven Science and Engineering:*  
1134 *Machine Learning, Dynamical Systems, and Control*. Cambridge Univer-  
1135 sity Press, ??? (2019)
- 1136 [41] Benner, P., Gugercin, S., Willcox, K.: A survey of projection-based model  
1137 reduction methods for parametric dynamical systems. *SIAM review*  
1138 **57**(4), 483–531 (2015)
- 1139 [42] Peherstorfer, B., Willcox, K.: Data-driven operator inference for nonin-  
1140 trusive projection-based model reduction. *Computer Methods in Applied*  
1141 *Mechanics and Engineering* **306**, 196–215 (2016)
- 1142 [43] Brunton, S.L., Proctor, J.L., Kutz, J.N.: Discovering governing equations  
1143 from data by sparse identification of nonlinear dynamical systems.  
1144 *Proceedings of the National Academy of Sciences* **113**(15), 3932–3937  
1145 (2016)
- 1146 [44] Loiseau, J.-C., Brunton, S.L.: Constrained sparse Galerkin regression.  
1147 *Journal of Fluid Mechanics* **838**, 42–67 (2018)
- 1148 [45] Qian, E., Kramer, B., Peherstorfer, B., Willcox, K.: Lift & learn: Physics-  
1149 informed machine learning for large-scale nonlinear dynamical systems.

- 1150           Physica D: Nonlinear Phenomena **406**, 132401 (2020)
- 1151 [46] Armanini, C., Farman, M., Calisti, M., Giorgio-Serchi, F., Stefanini,  
1152 C., Renda, F.: Flagellate underwater robotics at macroscale: Design,  
1153 modeling, and characterization. *IEEE Transactions on Robotics* (2021)
- 1154 [47] Dowell, E.H., Hall, K.C.: Modeling of fluid-structure interaction. *Annual*  
1155 *review of fluid mechanics* **33**(1), 445–490 (2001)
- 1156 [48] Hou, G., Wang, J., Layton, A.: Numerical methods for fluid-structure  
1157 interaction—a review. *Communications in Computational Physics* **12**(2),  
1158 337–377 (2012)
- 1159 [49] Souli, M., Benson, D.J.: *Arbitrary Lagrangian Eulerian and Fluid-*  
1160 *structure Interaction: Numerical Simulation*. John Wiley & Sons, ???  
1161 (2013)
- 1162 [50] Mittal, R., Iaccarino, G.: Immersed boundary methods. *Annu. Rev. Fluid*  
1163 *Mech.* **37**, 239–261 (2005)
- 1164 [51] Taira, K., Colonius, T.: The immersed boundary method: a projection  
1165 approach. *Journal of Computational Physics* **225**(2), 2118–2137 (2007)
- 1166 [52] Goza, A., Colonius, T.: A strongly-coupled immersed-boundary formu-  
1167 lation for thin elastic structures. *Journal of Computational Physics* **336**,  
1168 401–411 (2017)
- 1169 [53] Dickinson, M.H., Farley, C.T., Full, R.J., Koehl, M., Kram, R., Lehman,  
1170 S.: How animals move: an integrative view. *science* **288**(5463), 100–106  
1171 (2000)
- 1172 [54] Lauder, G.V.: Fish locomotion: recent advances and new directions.  
1173 *Annual review of marine science* **7**, 521–545 (2015)
- 1174 [55] FLOW3D software. <https://www.flow3d.com>. Accessed: 2021-10-27
- 1175 [56] Adina software. <http://www.adina.com>. Accessed: 2021-10-27
- 1176 [57] Weller, H.G., Tabor, G., Jasak, H., Fureby, C.: A tensorial approach to  
1177 computational continuum mechanics using object-oriented techniques.  
1178 *Computers in physics* **12**(6), 620–631 (1998)
- 1179 [58] Renda, F., Giorgio-Serchi, F., Boyer, F., Laschi, C., Dias, J., Seneviratne,  
1180 L.: A unified multi-soft-body dynamic model for underwater soft robots.  
1181 *The International Journal of Robotics Research* **37**(6), 648–666 (2018).  
1182 <https://doi.org/10.1177/0278364918769992>
- 1183 [59] Duraisamy, K., Iaccarino, G., Xiao, H.: Turbulence modeling in the age

- 1184 of data. *Annual Reviews of Fluid Mechanics* **51**, 357–377 (2019)
- 1185 [60] Brunton, S.L., Noack, B.R., Koumoutsakos, P.: Machine learning for  
1186 fluid mechanics. *Annual Review of Fluid Mechanics* **52**, 477–508 (2020)
- 1187 [61] Vinuesa, R., Brunton, S.L.: The potential of machine learning to enhance  
1188 computational fluid dynamics. arXiv preprint arXiv:2110.02085 (2021)
- 1189 [62] Bar-Sinai, Y., Hoyer, S., Hickey, J., Brenner, M.P.: Learning data-  
1190 driven discretizations for partial differential equations. *Proceedings of  
1191 the National Academy of Sciences* **116**(31), 15344–15349 (2019)
- 1192 [63] Kochkov, D., Smith, J.A., Alieva, A., Wang, Q., Brenner, M.P., Hoyer,  
1193 S.: Machine learning accelerated computational fluid dynamics. arXiv  
1194 preprint arXiv:2102.01010 (2021)
- 1195 [64] Wang, R., Walters, R., Yu, R.: Incorporating symmetry into deep dynam-  
1196 ics models for improved generalization. arXiv preprint arXiv:2002.03061  
1197 (2020)
- 1198 [65] Li, Z., Kovachki, N., Azizzadenesheli, K., Liu, B., Bhattacharya, K., Stu-  
1199 art, A., Anandkumar, A.: Fourier neural operator for parametric partial  
1200 differential equations. arXiv preprint arXiv:2010.08895 (2020)
- 1201 [66] Ling, J., Kurzawski, A., Templeton, J.: Reynolds averaged turbulence  
1202 modelling using deep neural networks with embedded invariance. *Journal  
1203 of Fluid Mechanics* **807**, 155–166 (2016)
- 1204 [67] Maulik, R., San, O., Rasheed, A., Vedula, P.: Subgrid modelling for  
1205 two-dimensional turbulence using neural networks. *Journal of Fluid  
1206 Mechanics* **858**, 122–144 (2019)
- 1207 [68] Novati, G., de Laroussilhe, H.L., Koumoutsakos, P.: Automating turbu-  
1208 lence modelling by multi-agent reinforcement learning. *Nature Machine  
1209 Intelligence* **3**(1), 87–96 (2021)
- 1210 [69] Beetham, S., Capecelatro, J.: Formulating turbulence closures using  
1211 sparse regression with embedded form invariance. *Physical Review Fluids*  
1212 **5**(8), 084611 (2020)
- 1213 [70] Beetham, S., Fox, R.O., Capecelatro, J.: Sparse identification of mul-  
1214 tiphase turbulence closures for coupled fluid–particle flows. *Journal of  
1215 Fluid Mechanics* **914** (2021)
- 1216 [71] Taira, K., Brunton, S.L., Dawson, S., Rowley, C.W., Colonius, T., McK-  
1217 eon, B.J., Schmidt, O.T., Gordeyev, S., Theofilis, V., Ukeiley, L.S.:  
1218 Modal analysis of fluid flows: An overview. *AIAA Journal* **55**(12),

- 1219 4013–4041 (2017)
- 1220 [72] Loiseau, J.-C., Noack, B.R., Brunton, S.L.: Sparse reduced-order mod-  
1221 eling: sensor-based dynamics to full-state estimation. *Journal of Fluid*  
1222 *Mechanics* **844**, 459–490 (2018)
- 1223 [73] Deng, N., Noack, B.R., Morzynski, M., Pastur, L.R.: Low-order model for  
1224 successive bifurcations of the fluidic pinball. *Journal of fluid mechanics*  
1225 **884**(A37) (2020)
- 1226 [74] Deng, N., Noack, B.R., Morzyński, M., Pastur, L.R.: Galerkin force  
1227 model for transient and post-transient dynamics of the fluidic pinball.  
1228 *Journal of Fluid Mechanics* **918** (2021)
- 1229 [75] Lee, K., Carlberg, K.T.: Model reduction of dynamical systems on  
1230 nonlinear manifolds using deep convolutional autoencoders. *Journal of*  
1231 *Computational Physics* **404**, 108973 (2020)
- 1232 [76] Raissi, M., Perdikaris, P., Karniadakis, G.E.: Physics-informed neural  
1233 networks: A deep learning framework for solving forward and inverse  
1234 problems involving nonlinear partial differential equations. *Journal of*  
1235 *Computational Physics* **378**, 686–707 (2019)
- 1236 [77] Lu, L., Jin, P., Pang, G., Zhang, Z., Karniadakis, G.E.: Learning non-  
1237 linear operators via deepnet based on the universal approximation  
1238 theorem of operators. *Nature Machine Intelligence* **3**(3), 218–229 (2021)
- 1239 [78] Shi, G., Shi, X., O’Connell, M., Yu, R., Azizzadenesheli, K., Anand-  
1240 kumar, A., Yue, Y., Chung, S.-J.: Neural lander: Stable drone landing  
1241 control using learned dynamics. In: 2019 International Conference on  
1242 Robotics and Automation (ICRA), pp. 9784–9790 (2019). IEEE
- 1243 [79] Johnson, K.L., Johnson, K.L.: *Contact Mechanics*. Cambridge university  
1244 press, ??? (1987)
- 1245 [80] Vakis, A.I., Yastrebov, V.A., Scheibert, J., Nicola, L., Dini, D., Minfray,  
1246 C., Almqvist, A., Paggi, M., Lee, S., Limbert, G., *et al.*: Model-  
1247 ing and simulation in tribology across scales: An overview. *Tribology*  
1248 *International* **125**, 169–199 (2018)
- 1249 [81] Dalvi, S., Gujrati, A., Khanal, S.R., Pastewka, L., Dhinojwala, A.,  
1250 Jacobs, T.D.: Linking energy loss in soft adhesion to surface roughness.  
1251 *Proceedings of the National Academy of Sciences* **116**(51), 25484–25490  
1252 (2019)
- 1253 [82] Studer, C., Glocker, C.: Simulation of non-smooth mechanical systems  
1254 with many unilateral constraints. *Proceedings ENOC-2005 Eindhoven*



- 1255 (2005)
- 1256 [83] Acary, V.: Projected event-capturing time-stepping schemes for non-  
1257 smooth mechanical systems with unilateral contact and coulomb’s  
1258 friction. *Computer Methods in Applied Mechanics and Engineering* **256**,  
1259 224–250 (2013)
- 1260 [84] Coevoet, E., Escande, A., Duriez, C.: Optimization-based inverse model  
1261 of soft robots with contact handling. *IEEE Robotics and Automation*  
1262 *Letters* **2**(3), 1413–1419 (2017)
- 1263 [85] Collins, J., Chand, S., Vanderkop, A., Howard, D.: A review of physics  
1264 simulators for robotic applications. *IEEE Access* (2021)
- 1265 [86] sofa framework. <https://www.sofa-framework.org>. Accessed: 2021-11-22
- 1266 [87] Xu, J., Aykut, T., Ma, D., Steinbach, E.: 6dls: Modeling nonplanar  
1267 frictional surface contacts for grasping using 6-d limit surfaces. *IEEE*  
1268 *Transactions on Robotics* (2021)
- 1269 [88] Xydas, N., Kao, I.: Modeling of contact mechanics and friction limit  
1270 surfaces for soft fingers in robotics, with experimental results. *The*  
1271 *International Journal of Robotics Research* **18**(9), 941–950 (1999)
- 1272 [89] Majidi, C., Shepherd, R.F., Kramer, R.K., Whitesides, G.M., Wood,  
1273 R.J.: Influence of surface traction on soft robot undulation. *The Inter-*  
1274 *national Journal of Robotics Research* **32**(13), 1577–1584 (2013)
- 1275 [90] Todorov, E., Erez, T., Tassa, Y.: Mujoco: A physics engine for  
1276 model-based control. In: 2012 IEEE/RSJ International Conference on  
1277 Intelligent Robots and Systems, pp. 5026–5033 (2012). IEEE
- 1278 [91] Deimel, R., Brock, O.: A novel type of compliant and underactu-  
1279 ated robotic hand for dexterous grasping. *The International Journal of*  
1280 *Robotics Research* **35**(1-3), 161–185 (2016)
- 1281 [92] Lipson, H., Pollack, J.B.: Automatic design and manufacture of robotic  
1282 lifeforms. *Nature* **406**(6799), 974–978 (2000)
- 1283 [93] Hiller, J., Lipson, H.: Automatic design and manufacture of soft robots.  
1284 *IEEE Transactions on Robotics* **28**(2), 457–466 (2011)
- 1285 [94] Coevoet, E., Escande, A., Duriez, C.: Soft robots locomotion and manip-  
1286 ulation control using fem simulation and quadratic programming. In:  
1287 2019 2nd IEEE International Conference on Soft Robotics (RoboSoft),  
1288 pp. 739–745 (2019)
- 1289 [95] Hwangbo, J., Lee, J., Dosovitskiy, A., Bellicoso, D., Tsounis, V., Koltun,

- 1290 V., Hutter, M.: Learning agile and dynamic motor skills for legged robots.  
1291 *Science Robotics* **4**(26) (2019)
- 1292 [96] Golemo, F., Taiga, A.A., Courville, A., Oudeyer, P.-Y.: Sim-to-real trans-  
1293 fer with neural-augmented robot simulation. In: *Conference on Robot*  
1294 *Learning*, pp. 817–828 (2018). PMLR
- 1295 [97] Battaglia, P., Pascanu, R., Lai, M., Jimenez Rezende, D., et al.: Interac-  
1296 tion networks for learning about objects, relations and physics. *Advances*  
1297 *in neural information processing systems* **29** (2016)
- 1298 [98] Jiang, Y., Liu, K.: Data-augmented contact model for rigid body  
1299 simulation (2018)
- 1300 [99] Sundaram, S., Kellnhofer, P., Li, Y., Zhu, J.-Y., Torralba, A., Matusik,  
1301 W.: Learning the signatures of the human grasp using a scalable tactile  
1302 glove. *Nature* **569**(7758), 698–702 (2019)
- 1303 [100] Lipson, H.: Challenges and opportunities for design, simulation, and  
1304 fabrication of soft robots. *Soft Robotics* **1**(1), 21–27 (2014)
- 1305 [101] Calisti, M., Laschi, C.: Morphological and control criteria for self-stable  
1306 underwater hopping. *Bioinspiration & biomimetics* **13**(1), 016001 (2017)
- 1307 [102] Chenevier, J., González, D., Aguado, J.V., Chinesta, F., Cueto, E.:  
1308 Reduced-order modeling of soft robots. *PloS one* **13**(2), 0192052 (2018)
- 1309 [103] Full, R.J., Koditschek, D.E.: Templates and anchors: neuromechanical  
1310 hypotheses of legged locomotion on land. *Journal of experimental biology*  
1311 **202**(23), 3325–3332 (1999)
- 1312 [104] Picardi, G., Chellapurath, M., Iacoponi, S., Stefanni, S., Laschi, C., Cal-  
1313 ista, M.: Bioinspired underwater legged robot for seabed exploration with  
1314 low environmental disturbance. *Science Robotics* **5**(42) (2020)
- 1315 [105] Bujard, T., Giorgio-Serchi, F., Weymouth, G.D.: A resonant squid-  
1316 inspired robot unlocks biological propulsive efficiency. *Science Robotics*  
1317 **6**(50), 2971 (2021). <https://doi.org/10.1126/scirobotics.abd2971>